Copyright Warning & Restrictions

The copyright law of the United States (Title 17, United States Code) governs the making of photocopies or other reproductions of copyrighted material.

Under certain conditions specified in the law, libraries and archives are authorized to furnish a photocopy or other reproduction. One of these specified conditions is that the photocopy or reproduction is not to be "used for any purpose other than private study, scholarship, or research." If a, user makes a request for, or later uses, a photocopy or reproduction for purposes in excess of "fair use" that user may be liable for copyright infringement,

This institution reserves the right to refuse to accept a copying order if, in its judgment, fulfillment of the order would involve violation of copyright law.

Please Note: The author retains the copyright while the New Jersey Institute of Technology reserves the right to distribute this thesis or dissertation

Printing note: If you do not wish to print this page, then select "Pages from: first page # to: last page #" on the print dialog screen

ABSTRACT

LONG TERM RISK ASSESSMENT OF BROWNFIELD CONTAINMENTS

by
Shailesh Chirputkar

The sites at which the development is hindered by real or perceived contamination are called as Brownfield sites. It is a common trend in industry to develop these types of sites with surface and peripheral containments. It might prove unwise to develop the sites in this manner from a long term perspective without considering the associated risk. Because of this, a model has been proposed for long term risk assessments of brownfield containments.

Objectives of this study were to develop a contaminant transport model for flow of contaminants towards the surface and peripheral containments inside the site, a model for flow of contaminants through the containments and calculate the risk using CalTOX model.

The model consists of two parts i.e. flow of contaminants towards peripheral containments and surface containments. The flow of contaminants towards surface containments is based on a process based model and flow of contaminant towards surface containments is based on Richard's equation. The peripheral containment model was applied to three case histories. The risk was acceptable in one case, unacceptable in another case and on the borderline in the third case. Thus the model was able to project the risk towards long term scenario.

Flow of contaminants towards surface containments in the vadoze zone can be modeled by Richard's equation that is a nonlinear, transient, partial differential equation

of parabolic type. The equation was solved using the finite difference technique. The surface containment model was applied to a fictitious site and to a real case involving hexavalent chromium contamination. The model was able to predict the flow of contaminants in the vadoze zone. Risk was calculated using CalTOX model with modified fugacity approach.

CalTOX model utilized for risk, in the original form utilizes only residential exposure scenarios and only for organic chemicals. This model was modified to incorporate industrial exposure factors and inorganic chemicals.

LONG TERM RISKS ASSOCIATED WITH BROWNFIELD CONTAINMENTS

by
Shailesh Shirish Chirputkar

A Dissertation
Submitted to the Faculty of
New Jersey Institute of Technology
in Partial Fulfillment of the Requirements for the Degree of
Doctor of Philosophy

Department of Civil and Environmental Engineering

May 1999

APPROVAL PAGE

LONG TERM RISKS ASSOCIATED WITH BROWNFIELD CONTAINMENTS

Shailesh Shirish Chirputkar

Dr. Dorairaja Raghu, Dissertation Advisor — Date
Professor of Civil and Environmental Engineering, NJIT

Dr. William Spillers, Committee Member — Date
Distinguished Professor of Civil and Environmental Engineering, NJIT

Dr. Jay N. Meegoda, Committee Member — Date
Associate Professor of Civil and Environmental Engineering, NJIT

Dr. Manish Bhattacharjee, Committee Member — Date
Professor of Mathematical Sciences, NJIT

William Librizzi, Committee Member — Date
Director of Technology Applications, Center for Env. Engg. and Sciences, NJIT

BIOGRAPHICAL SKETCH

Author: Shailesh Shirish Chirputkar

Degree: Doctor of Philosophy

Date: May 1999

Undergraduate and Graduate Education:

- Doctor of Philosophy in Civil Engineering
  New Jersey Institute of Technology, Newark, NJ, 1999
- Master of Science in Civil Engineering,
  Indian Institute of Technology, Kanpur, India, 1995
- Bachelor of Science in Civil Engineering,
  University of Pune, Pune, India, 1993.

Major: Civil Engineering

Presentations and Publications:

1. S.S. Chirputkar and D. Raghu, 1997. "Applications of Knowledge Based System in Bioremediation", *International Conference on Solid Waste Management*, Philadelphia.

2. D. Raghu and S.S. Chirputkar, 1997. "Innovative Treatment of Contaminated Soils" *ASCE Special Technical Publication*, QA/QC Procedures.

3. S.S. Chirputkar and D. Raghu, 1998. "Risk Evaluation in Brownfield Slurry Wall Containments by Contaminant Transport and CalTOX models", *ASCE Special Technical Publication on Brownfields*.

4. S.S. Chirputkar and D. Raghu, 1998. "A Contaminant Transport Model for Determining Risk Due to Containments in Brownfields", *International Conference on Solid Waste Management*, Philadelphia.

To my beloved family and spiritual teacher

ACKNOWLEDGEMENT

I would like to express my deepest appreciation to Dr. Dorairaja Raghu, who not only served as my research supervisor, providing valuable and countless resources, insight, and intuition, but also constantly gave me support, encouragement and reassurance. Special thanks are given to Prof. William Librizzi, Dr. William Spillers, Dr. Manish Bhattacharjee and Dr. Jay Meegoda for actively participating in my doctoral research.

I also wish to thank Dr. Sudhi Mukherjee, Dr. Gerry McKenna and Dr. Khera for their assistance over years.

I am grateful to Civil and Environmental Engineering for providing me the assistantship and resources for the research.

Many of my fellow graduate students in the department, especially Swamy Basim, Wiwat and Lansagna are deserving their support.

TABLE OF CONTENTS

Chapter **Page**

1. INTRODUCTION AND STATEMENT OF THE PROBLEM.....1

1.1 Introduction.....1

1.2 Statement of the Problem.....1

1.3 Scope of this Study.....5

2. LITERATURE REVIEW.....7

2.1 Introduction 7

2.2 Brownfields Development.....7

2.3 Different Models Available for Risk Assessment.....7

2.4 CalTOX Model and Risk Calculation.....8

2.4.1 Risk Calculation.....9

2.5 Risk Assessment Procedures.....11

2.6 Statistical Approach to Clean Up Goals.....14

2.7 Contaminant Transport Models.....14

2.8 Containment and Capping.....15

2.9 Flow towards Caps.....17

2.9.1 Flow Towards Caps.....18

2.9.2 Flow through Caps.....18

3. DEVELOPMENT OF MODEL FLOW FOR TOWARDS AND THROUGH PERIPHERAL CONTAINMENTS.....19

3.1 Introduction.....19

Chapter **Page**

3.2 Contaminant Transport Model for Flow towards and through the Peripheral Containment.....19

3.3 Transport Model.....20

3.4 Advection Process.....21

3.4.1 Point Sources vs. Concentration Contours.....23

3.4.2 Multiple Point Sources.....23

3.4.3 Travel Time from Source to Wall.....23

3.5 Diffusion Process.....24

3.6 Determination of Concentrations at the Outer Face of the Wall.....24

3.7 Determination of Risk/Hazard Ratio.....28

4. DEVELOPMENT OF MODEL FOR SURFACE CONTAINMENTS.....29

4.1 Introduction.....29

4.2 Contaminant Transport Model for Flow Towards and Through the Surface Containments.....29

4.3 Flow of Contaminants in Capillary Zone.....30

4.4 Richard's Equation.....31

4.5 Solution of Richard's Equation.....32

4.5.1 Prior Work Done in Solving Richard's Equation.....34

4.5.2 Formulation of Richard's Equation.....35

4.5.3 Choice of Time Step.....36

4.5.4 Determination of Soil Parameters.....37

4.5.5 Finite Difference Schemes.....37

Chapter **Page**

4.5.5.1 Forward Difference Scheme.....37

4.5.5.2 Predictor Corrector Method.....37

4.6 Calculation of Contaminant Concentration.....38

4.7 Installation of a Gravel Bed.....38

4.8 Determination of Risk/Hazard Ratio.....39

4.8.1 Determination of Risk Due to Chromium Contamination.....39

5. RESULTS AND DISCUSSIONS FOR FLOW TOWARDS AND THROUGH PERIPHERAL CONTAINMENTS.....41

5.1 Introduction.....41

5.2 Case Study No. 1.....41

5.2.1 Site Description.....41

5.2.2 Seepage Velocity.....43

5.2.3 Source Concentration.....43

5.2.4 Chemical Gradient.....44

5.2.5 Determination of Concentration at Inner Face of Wall.....45

5.2.6 Determination of Concentrations at the Outer Face of the Wall.....46

5.2.7 Determination of Risk/Hazard Index.....49

5.3 Case Study No. 2.....49

5.3.1 Site Description.....49

5.3.2 Seepage Velocity.....50

5.3.3 Source Concentrations.....52

5.3.4 Contaminant Concentration at Inner Surface.....52

Chapter **Page**

5.3.5 Determination of Contaminant Concentration at Outer Surface for Multiple Point Sources....53

5.3.6 Determination of Risk/Hazard Ratio for Multiple Point Sources....54

5.4 Case Study No. 3: Galloway Township Site....56

5.4.1 Site Description....56

5.4.2 Seepage Velocity....57

5.4.3 Source Concentration....57

5.4.4 Chemical Gradient....58

5.4.5 Contaminant Concentration at Inner Surface....58

5.4.6 Contaminant Concentration at Outer Surface....59

5.4.7 Calculation of Risk/Hazard Ratio....61

6. RESULTS AND DISCUSSIONS FOR FLOW TOWARDS AND THROUGH SURFACE CONTAINMENTS....63

6.1. Preamble....63

6.2. Case study number 1....63

6.2.1. Introduction....63

6.2.2. Input Data for the Program....63

6.2.3 Results Obtained and Discussion of results....66

6.2.3.1 Effect of Diffusivity on Results....68

6.2.3.2 Effect of $\Delta z/h$ on results....69

6.3 Case Study No. 2....73

6.3.1 Site Description....73

6.3.2 Input File....74

Chapter **Page**

6.3.3 Results Obtained and Discussion of Results....75

6.3.4 Calculation of Risk....78

6.4 Strategies for Development based on Model....79

7. CONCLUSION....81

7.1 Conclusion....81

7.2 Recommendation for Future Study....82

APPENDIX A DERIVATIONS....83

APPENDIX B FINITE DIFFERENCE FORMULATION FOR SOLUTION OF RICHARD'S EQUATION....85

APPENDIX C MODIFIED FUGACITY EQUATIONS....88

REFERENCES....90

LIST OF FIGURES

Figure **Page**

1.1 Active Containment at a Contaminated Site....4

1.2 Passive Containment at a Contaminated Site....5

2.1 Baseline Risk Assessment....12

3.1 Process Tree for Contaminant to Travel to the Face of the Wall and for the Flow of Contaminant Through the Wall/Cap....21

3.2 Seepage Velocity vs. Time for Cl-....22

3.3Concentration vs. Time for Cl-....22

3.4 G(t) vs. Time (Calculated from data provided by Anderson)....25

3.5 G(t) vs. Time (Calculated from data provided by Anderson)....25

3.6 Wall Functions....27

4.1 Process Tree for Contaminant to Travel to the Face of the Wall and for the Flow of Contaminant Through the Cap....30

4.2 Concentration of Contaminant at Inner Surface of Surface Containment vs. Time....40

4.3 Risk vs. Time at Inner Surface of Surface Containment vs. Time....40

5.1 Schematic Diagram of Site for Case Study No. 1....41

5.2 Seepage Velocity vs. Time Considered for This Study....43

5.3 Concentration vs. Time Considered for Study....44

5.4 Chemical Gradient vs. Time Plot Utilized for Present Study....45

5.5 Contaminant Concentration at the Inner Surface of Containment vs. Time....45

5.6 Concentration of Contaminant, Carried Away from Face of Wall (High Permeability Soil)....47

5.7 Concentration of Contaminant, Accumulating at Outer Face of Wall (Low Permeability Soil)....47

Figure **Page**

5.8 Hazard Index at Outer Face of Wall, Contaminant Carried Away from Face of Wall (High Permeability Soil)....48

5.9 Hazard Index at Outer Face of Wall, Contaminant Accumulating at Outer Face of Wall (Low Permeability Soil)....48

5.10 Schematic Representation of Site....50

5.11 Seepage Velocity vs. Time (After Barry et. al., 1997)....51

5.12 Concentration vs. Time for TCE Source 1, 2, 3, 4....52

5.13 Contaminant Concentration at Inner Face of Wall....53

5.14 Contaminant with Multiple Point Sources Carried Away from the Face of the Wall (High Permeability Soil) with Bad Construction....54

5.15 Contaminant with Multiple Point Sources Accumulating at the Face of the Wall (Low Permeability Soil) with Bad Construction....54

5.16 Cancer Risk vs. Time (Contaminant Carried Away from Outer Face of the Wall)....55

5.17 Cancer Risk vs. Time (Contaminant Accumulating at Outer Face of the Wall)....55

5.18 Schematic Diagram of Galloway Township Site....56

5.19 Seepage Velocity vs. Time (Galloway Township)....57

5.20 Leaked Contaminant vs. Time....58

5.21 Source Concentration vs. Time....58

5.22 Contaminant Concentration at the Inner Face of the Wall....59

5.23 Contaminant Concentration vs. Time, Contaminant Carried Away from the Face of the Wall with Bad Construction....59

5.24 Contaminant Concentration vs. Time, Contaminant Accumulating at the Face of the Wall with Bad Construction....60

5.25 Contaminant Concentration vs. Time, Contaminant Accumulating at the Outer Face of the Wall with Good Construction....60

Figure **Page**

5.26 Contaminant Concentration vs. Time, Contaminant Carried Away from the Outer Face of the Wall with Good Construction....60

5.27 Cancer Risk vs. Time for Contaminant Carried Away from the Face of the Wall with Bad Construction....61

5.28 Cancer Risk vs. Time for Contaminant Accumulating at the Face of the Wall with Bad Construction....61

5.29 Cancer Risk vs. Time for Contaminant Carried Away from the Face of the Wall with Good Construction....61

5.30 Cancer Risk vs. Time for Contaminant Accumulating at the Face of the Wall with Good Construction....62

6.1 Depth vs. Water Content for Sand....71

6.2 Depth vs. Water Content for Silt....72

6.3 Depth vs. Water Content for Clay....72

6.4 Subsurface Profile for Case Study No. 2....74

6.5 Depth vs. Water Content for Case Study No. 2....76

6.6 Volumetric Water Content vs. Time....77

6.7 Concentration vs. Time for Case Study No. 2....78

6.8 Risk vs. Time for Case Study Number 2....79

LIST OF TABLES

Table **Page**

2.1 Industrial Exposure Scenarios....12

4.1 Types of Partial Differential Equation....33

6.1 Input File for Sand....64

6.2 Input Data for Silt....64

6.3 Input Data for Clay....65

6.4 The Time for Maximum Capillary Rise Obtained from the Results and Corresponding Values Computed from Terzaghi's Equation, Predictor Corrector Method, Forward Difference Method....67

6.5 Effect of Diffusivity Volumetric Water Content on Sand at t. = 1.03 68

6.6 Effect of Diffusivity Volumetric Water Content on Silt at t = 99 Days....68

6.7 Effect of Diffusivity Volumetric Water Content on Clay at t = 2187 Days....68

6.8 Volumetric Water Content at the Top of Capillary Surface for Sands After 1.03 Hours....69

6.9 Volumetric Water Content at the Top of Capillary Surface for Silts after 99 Days....70

6.10 Volumetric Water Content at the Top of Capillary Surface for Clays After 2187 Days....70

6.11 Water Content Profile for Sand at Diffusivity = 0.125 and $\Delta z/h = 0.17$....71

6.12 Water Content Profile for Silt at Diffusivity = 0.125 and $\Delta z/h = 0.17$....71

6.13 Water Content Profile for Clay at Diffusivity = 0.125 and $\Delta z/h = 0.17$....72

6.14 Input File for Case History Number 2....74

6.15 Effect of Diffusivity on Volumetric Water Content After 1.03 Hours....75

Table **Page**

6.16 Volumetric Water Content at the Top of Capillary Surface for Case Study No. 2 After 1.03 Hours.....76

6.17 Volumetric Water Content Profile for Diffusivity = 0.125 and $\Delta z/h = 0.17$.....77

LIST OF SYMBOLS, ABBREVIATIONS AND ACRONYMS

A_l =Area of a Subarea Within a Contour

ARAR = Applicable or Relevant and Appropriate Regulations

C= Concentration of a Chemical Measured in Terms of Moles

C(t) = Concentration of a Contaminant at a Given Instant of Time

$C_a(t)$ = Contaminant Concentration Due to Advection Process which Is a Function of Time.

$C_d(t)$ = Concentration of a Contaminant in Diffusion Process Which Is a Function of Time.

$C_i(t)$ = Concentration of a Contaminant on Inside Face of a Slurry Wall as a Function of Time.

C_l = Concentration of a Subarea Within a Contour

C_o = Initial Concentration of Contaminant

$C_o(t)$ = Concentration of a Contaminant on Outside Face of a Slurry Wall as a Function of Time.

C_v = Coefficient of Consolidation

$C_w(h)$ = Water Capacity Function

C(t) = Source Concentration Which is a Given Function of Time

CERCLA = Comprehensive Environmental Response, Compensation Liability Act

d = Distance Traveled by a Contaminant

$D_w(\theta)$ = Soil Water Diffusivity

D_{10} = Diameter at 10% Passing.

D^* = Apparent Diffusion Coefficient

D^o = Pure Diffusion Coefficient

e = Void Ratio

e_0 = Initial Void Ratio of the Slurry Wall

e(t) = Void Ratio of Slurry Wall

EPA = Environmental Protection Agency

f = Fugacity Measured in Terms of Pascal

G(t) = Chemical Gradient of a Contaminant Which is a Function of Time.

$G_{max.}$ = Maximum Value of Contaminant Gradient at a Given Location from a Given Source

h = Matrix Suction

ho = Initial Thickness of Slurry Wall

h = Normalized Matric Suction

h(t) = Thickness of Slurry Wall

H = Maximum Value of Matric Suction

H_c = Capillary Head

I = Time Coordinate

J = Spatial Coordinate

k = Coefficient of Permeability

k = Normalized Permeability

K = Maximum Value of Permeability, Saturated Permeability

K_i = Stress intensity factor

K_{Di} = Sorption Coefficient is a Medium for a Particular Contaminant

$K(h)$ = Permeability of Soil Expressed as a Function of Matric Potential

$K(\theta)$ = Permeability of Soil as a Function of Water Content

M = Molecular Weight of the Compound

n = Porosity

n(t) = Porosity of the Wall Expressed as Function of Time.

N = Moles of a Gas

P = Pressure Exerted by a Gas.

R = Universal Gas Constant.

RBCA = Risk Based Corrective Action

t = Time Required for Meniscus of Capillary Water to Rise to the Height z Above the Free Water Level.

t_{μ} = Mean Time of Contaminant Travel

t_{σ} = Standard Deviation of Contaminant Travel Time

T = Absolute Temperature Measured in Kelvins

T(t) = Wall Function at Any Time t

TCE = Trichloroethylene

u = Pore Pressure

u_{xx} = Second Order Partial Derivative of a Function u with respect to x

u_{yx} = Second Order Partial Derivative of a Function u with respect to y

u_{yy} = Second Order Partial Derivative of a Function u with respect to x and y

u_{x} = First Order Partial Derivative of a Function u with respect to x

u_{y} = First Order Partial Derivative of a Function u with respect to y

USEPA = United States Environmental Protection Agency

USGS = United States Geological Survey

V = Volume Occupied by a Gas.

V_{o} = Initial Velocity of the Contaminant

$V_s(t)$ = Seepage Velocity Which is a Function of Time.

X_i = X coordinate of the Center of Gravity of a Subarea within a Concentration Contour

Y_i = Y Coordinate of the Center of Gravity of a Subarea within a Concentration Contour

z = Distance of Capillary Meniscus from Groundwater Level.

Z = Fugacity Capacity Expressed in Terms of Concentration per Unit Energy.

Z_{air} = Fugacity Capacity of Air

GREEK SYMBOLS

α = A Parameter Obtained by Curve Fitting

β = A Parameter Obtained by Curve Fitting

θ = Volumetric Water Content

θ_f = Final Water Content

θ_i = Initial Water Content

ρ_{si} = Density of a Medium.

τ = Tortuosity

Δt = Time Increment

Δz = Space Increment

$\Delta \mathbf{z}$ = Normalized Increment in Space i.e. a Ratio of Increment in Space to Maximum Capillary Rise.

CHAPTER 1

INTRODUCTION AND STATEMENT OF THE PROBLEM

1.1 Introduction

There are a number of sites across United States that once were used for industrial and commercial purposes and now have been abandoned or are underused. Such sites occupy respectively about 7000 acres and 25,000 acres of land in urban counties in New Jersey and United States respectively. Some of these sites are contaminated and/or perceived to be contaminated. If there is a potential for environmental concerns, industry and developers do not consider the site for development. This is due to the uncertainty of added costs or potential undefined future long-term liabilities. Such sites are called as Brownfield sites. In short, a Brownfield site can be defined as an abandoned, idled or under-used industrial and commercial site where expansion or redevelopment is complicated by real or perceived contamination. (USEPA, 1998a)

1.2 Statement of the Problem

There are major barriers legal, financial, practical, real or perceived that currently impede the developers from participating in and investing financial resources in the cleanup and redevelopment of the site that are or potentially subject to Superfund program and CERCLA (Comprehensive Environmental Response, Compensation Liability Act) program.

The stringency of EPA Superfund clean-up standards is often cited as major impediment to the cleanup and redevelopment of brownfield sites. Contaminated sites that are developed under Superfund program must meet standards known as ARARs ("Applicable or Relevant and Appropriate Regulations"). Also CERCLA prefers a remedial action in the form of treatment or elimination of the contaminants or reduction to a specified level in ARAR for each contaminant. Prospective developers state that the cost of meeting the stringent standards makes or may make the project economically infeasible. Though there are several other factors that dominate the decision to proceed or not to proceed in a particular project, the cost of remediation can be a dominating factor.

The stringent Superfund standards and preference for active treatment may be appropriate for cleaning up sites that are heavily contaminated and near residential areas where frequent human exposure is likely. Superfund standards are perceived as inappropriate for many brownfield sites that may or may not be seriously contaminated and where human and environmental exposure can be limited through various mechanisms. However, CERCLA and Superfund programs, as implemented, provide little flexibility to set alternative cleanup standards based on reasonable distinctions among the level of risk at each site based upon the severity of contamination and likelihood of human exposure to the contamination.

Though the regulatory agencies have stipulated cleanup standards for Superfund sites, the present regulatory trend is to utilize risk-based remediation. This is commonly referred to as RBCA (Risk Based Corrective Action). It is now possible for Brownfield sites to be cleaned up to standards far less stringent than those applied for Superfund sites. However, the stipulations of federal regulations such as RCRA (Resource

Conservation and Recovery Act) and CERCLA that make the owner responsible for possible risk in the long term from adverse effects resulting from contamination still apply. The higher the level of cleanup, the higher is the cost of cleanup and the lower the risk. The developer will have to make decisions regarding development taking the cost and risk into account.

Based on the authors' discussions with consultants and developers, it has been noted that the cheapest way of developing a Brownfield site is to contain it with bentonite slurry walls and asphalt caps. In this way, the time and expenses required for cleanup can be optimized. There are two types of peripheral containments that can be utilized. Figure 1.1 below shows a site with active containment consisting of a slurry wall and an asphalt cap. Plan shows hot spots of the contamination in the site. The pathways from a source to the containment are shown in the Figure. The structural integrity of the containment may be impaired in the long term not only by the chemical action between the contaminant and the containment material but also due to poor construction and cracking. An active containment is used to prevent contamination from escaping out of the Brownfield site.

A passive containment prevents contaminant from entering the development from an adjacent site. This is illustrated in Figure 1.2 where the sources of contamination are concentrated in one part of the site. The portion of the site that is highly contaminated is covered by asphalt cap and is separated from the remaining portion of the site by a slurry wall. Brownfield development, in this case, is on the portion of the site that is not contaminated or lightly contaminated. The contaminant may enter through the bentonite slurry wall or may escape through asphalt cap and cause problems for the development.

Thus in a Brownfield site either with an active or a passive containment, the contaminant will migrate to the surface and wall in time. As the containment deteriorates structurally with the passage of time, the contaminant will leak through the containment. If the contaminant flowing through the wall causes adverse effects, full or partial remediation to reduce leakage may be required. The degree of remediation will depend upon the acceptable risk. There are no tools available to estimate the concentrations of the contaminant coming out of the containment. For this purpose, a contaminant transport model will be developed in this study for an active containment. This model can also be used for a passive containment.

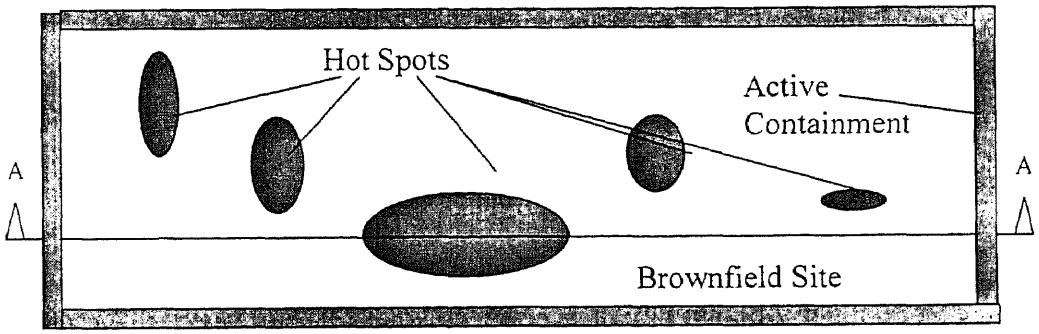

Plan of a Brownfield site

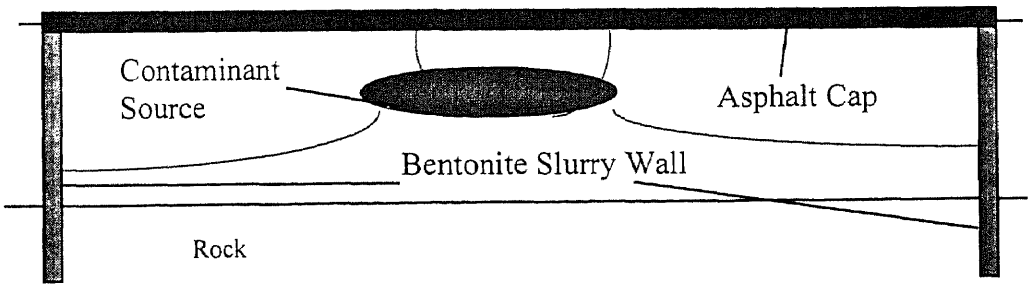

Section AA

Fig. 1.1 Active Containment at a Contaminated Site

1.3 Scope of this Study

For this study, it is proposed that long-term risks of a Brownfield site will be studied using contaminant transport and risk modeling. The scope of this study is as follows,

Develop a methodology for risk calculation in Brownfields for capping and containment.

(i) Develop a model for flow of contaminants in the site.

(ii) Develop a model for flow of contaminants through capping/containment.

(iii) Calculate the risk using CalTOX model.

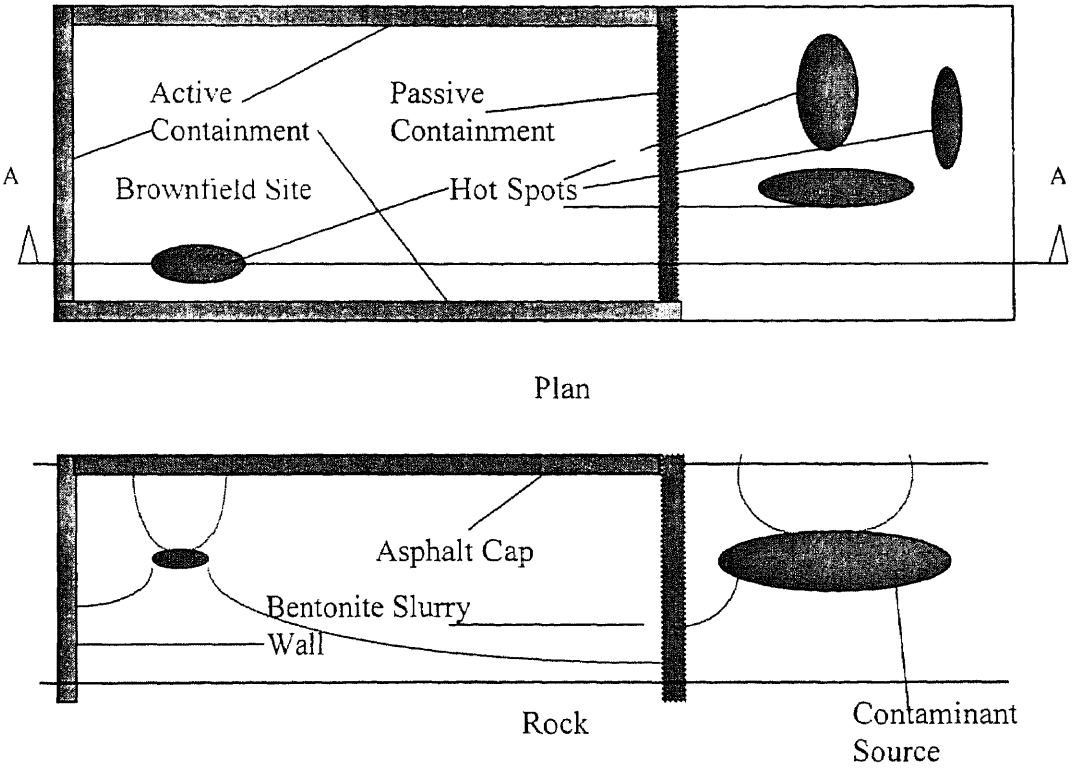

Fig. 1.2 Passive Containment at a Contaminated Site

In the following sections of this proposal, a brief review of available literature on this subject will be presented. This will be followed by a succinct discussion on the methodology to be adopted for this study.

Techniques for estimating the flow of contaminant towards and through wall were developed in this research. Results from case studies have been presented. For estimating the flow towards the surface containment, Richard's equation for flow through capillary zone was solved adopting finite difference formulations developed for this study. A case study for this condition has been presented. A methodology was outlined for determining long term risk utilizing CalTOX model based on flow data regarding the contaminants. In all case studies, various scenarios for possible development taking long term risk into account have been discussed.

CHAPTER 2

LITERATURE REVIEW

2.1 Introduction

In this chapter, relevant literature regarding Brownfields development will be discussed. Then available risk models such as CalTOX, their capabilities and limitations will be presented. Risk assessment procedures recommended by EPA will be reviewed. This will be followed by a discussion on the available contaminant transport models. After this, pertinent information regarding the containment and capping will be reviewed.

2.2 Brownfields Development

A very good discussion regarding Brownfields is provided in the Publication "Expediting Cleanup and Redevelopment of Brownfields- Addressing the major barriers to Private Sector real or Perceived" (USEPA, 1998b). Legislation regarding Brownfields was enacted in order to utilize the contaminated sites for meaningful and economically viable development while at the same time minimizing the effects of contamination on the surrounding environment. Brownfields are also subject to legislation that classifies the site as either a Groundwater Classification Exception area or Environmentally Restricted areas. In such cases, the use of land and/or groundwater is subject to certain restrictions.

2.3 Different Models Available for Risk Assessment

Various types of software are available in the industry, such as Hazard-Expert, Ramas-age, RBCA toolkit and CalTOX. Hazard-Expert can be used for processing and evaluating the expected hazardous effects of organic chemical compounds through

toxicokinetic and toxicodynamic investigation. Ramas-age can be used to analyze ecological risks of biological species. RBCA toolkit is a risk based correction analysis tool kit to carry out risk analysis according to ASTM and EPA procedures. CalTOX is developed by Department of Toxic Substances, California. The software has been utilized vastly in academic and industry circles. CalTOX has been selected for the present study for a number of reasons which are listed in next section. A review of the CalTOX model is presented in the following section.

2.4 CalTOX Model and Risk Calculation

Even though several models are available to carry out risk assessment, CalTOX model has been utilized for this study for a number of reasons. This model is an innovative spreadsheet model developed by the California Department of Toxic Substances. It computes the human health risks for a given concentration of a contaminant in a soil. The transport model in this package is intended for application over long time scales, several months to a decade. This model is intended for application over long time scales, several months to decades. It is not applicable for areas less than 1000 m^2 and greater than 10^7 m^2. CalTOX model is not suited for land plots having greater than 10% watershed area. Most of the Brownfield sites satisfy the above two criteria.

The CalTOX model has three main features, Multimedia transport and transportation model, Exposure Scenario models and Sensitivity and Uncertainty analysis. The multimedia transport and transformation model assesses time varying concentrations with constant input and uses equations based on conservation of mass and chemical equilibrium. It determines the chemical concentrations of contaminants in

various exposure media. From these concentrations, a daily intake of the contaminant is calculated. With daily intake and the corresponding toxicity data, the risk is calculated for the carcinogenic chemicals. For non-cancer causing chemicals, risk is expressed as Hazard Ratio. EPA calls it Hazard Index (EPA, 1989). CalTOX has the ability to carry out uncertainty analysis of the properties of contaminants used for risk analysis. These properties such as partition coefficients, Henry's constant, etc. are contained in the CalTOX software.

2.4.1 Risk Calculation

CalTOX model uses a concept based on fugacity for organic chemicals and a modified fugacity approach for inorganic chemicals, metals and radionuclides. Fugacity is a way of expressing concentration of chemicals.

$$C = f * Z \qquad (2.1)$$

Where,

C= Concentration of a chemical measured in terms of moles.

f = Fugacity measured in terms of Pascal

Z= Fugacity capacity expressed in terms of concentration per unit energy.

The physical interpretation of fugacity can be arrived at in the following manner:

The fugacity capacity in units of mol/m3-Pa for a nonionic organic chemical in pure air is given by,

$$Z_{air} = 1/(R\ T) \qquad (2.2)$$

Where,

Z_{air} = Fugacity Capacity in Air

R = Universal Gas Constant.

T = Absolute Temperature measured in Kelvins

The ideal gas equation is

$$PV = NRT \tag{2.3}$$

Where,

P = Pressure exerted by a gas.

V = Volume occupied by a gas.

N = moles of a gas

PV = capacity of a gas to perform the work, i.e. energy.

Hence,

$$1/RT = N/PV = Z_{air} \tag{2.4}$$

Fugacity capacity can be defined as the amount of energy required to change the concentration of a chemical. Hence the greater the amount of energy required to change the concentration of a chemical, the less mobile the chemical is. In other words, fugacity capacity is a measure of immobility of a chemical and fugacity is a measure of mobility of a chemical.

For nonionic organic chemicals the fugacity capacity in other mediums such as surface water, soil, ground water is calculated based upon the fugacity capacity of air. For ionic organic chemicals, inorganic chemicals, metals and radionuclides the fugacity capacity is calculated based upon the fugacity capacity in water. Mackay and Diamond (1989) define the fugacity capacity of water as 1 mol/m3-Pa as base. Based upon the

fugacity capacity in water, the fugacity capacity in other mediums can be calculated by using equation 2.5.

$$Z_{ip} = K_{Di} * \rho_{si} * Z_{water} * 1m^3/1000\ L\ water \qquad (2.5)$$

Where,

i = different compartments such as ground water, surface water, soil, sediments, plants, etc. and p corresponds to particle of each medium.

K_{Di} = sorption coefficient in a medium for a particular contaminant.

ρ_{si} = density of a medium.

Sorption coefficient in a medium can be calculated by using organic carbon content in a medium and organic carbon partition coefficient.

2.5 Risk Assessment Procedures

According to the Superfund Risk Assessment Manual (USEPA, 1989), risk assessment process consists of four main stages as shown in Figure 2.1. CalTOX model only considers residential exposure scenarios and thus does not address industrial exposure scenarios. Brownfield sites are usually developed for industrial purposes. Hence it is proposed that industrial exposure scenarios would be built in CalTOX to carry out quick assessment. One such industrial exposure scenario is given in Table 2.1 (CalTOX, 1998).

Toxicity assessment has been incorporated in the CalTOX model. Additional data regarding toxicity is available on http://www.tera.org (1998). CalTOX is capable of performing risk characterization. But it can only be performed for one contaminant at a time. USEPA procedures (USEPA, 1989) allow adding the risks for individual contaminants to

Figure No. 2.1

BASELINE RISK ASSESSMENT

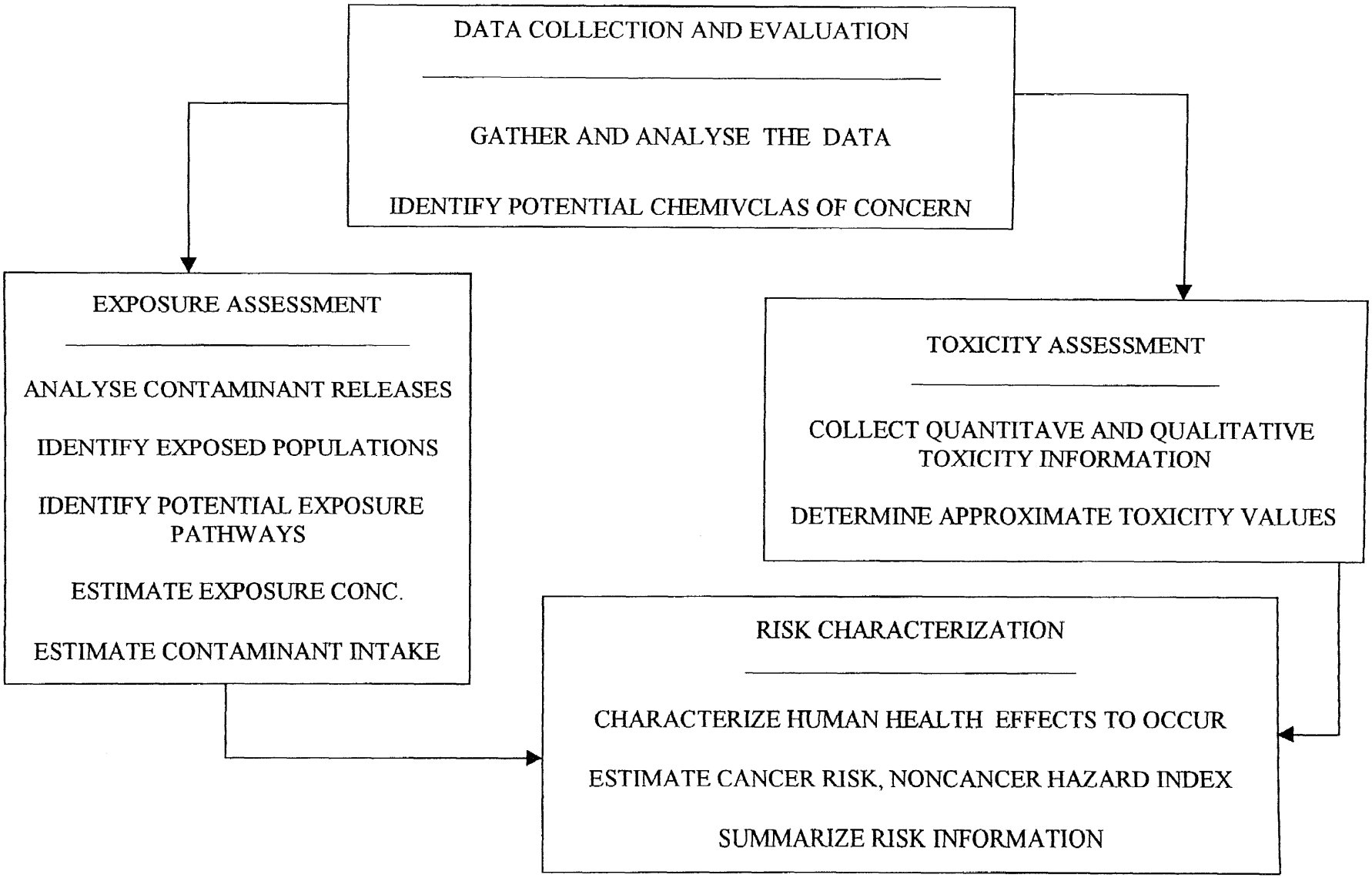

Table 2.1 Industrial Exposure Scenarios

Industrial	Exposure	Scenario				
Media	Exposure Route	Intake Rate	Exposure Freq.	Exposure Duration	Body Wt.	Averaging Time
Soil	Ingestion	50 mg/d	146	20	70	365*20
	Dermal	1 Contact/d	146	20	70	365*20
	Inhalation	20 m^3/d	146	20	70	365*20
Air	Inhalation	20 m^3/d	250	20	70	365*20
Ground water	Ingestion	1L/d	250	20	70	365*20
	Dermal		250	20	70	365*20
	Inhalation	20 m^3/d	250	20	70	365*20
Surface water	Ingestion	1L/d	250	20	70	365*20
	Dermal		250	20	70	365*20
	Inhalation	20 m^3/d	250	20	70	365*20

come up with a single cancer risk and/or noncancer hazard index for a particular site with a number of contaminants. Cleanup goals can be established based on risk in Brownfield sites.

2.6 Statistical Approach to Clean Up Goals

Pre-remediation concentrations can be represented as a lognormal distribution (Bowers et. al.(1996)). Response goal can be described by a function of geometric mean and geometric standard deviation of a lognormal distribution and desired reduction in exposure, which is defined as the ratio of average post-remediation concentration to average pre-remediation concentration. Exposure is always a function of the arithmetic mean concentration over a predefined exposure area, regardless of the type of distribution that best describes the contaminant concentration. Post remediation concentrations form a lognormal distribution. This post remediation distribution is truncated at a response goal with another distribution which represents the concentration of the contaminant in the backfill or cover. The average concentration of post remediation distribution is a weighted average of the portion of pre-remediation distribution with concentration below response goal and the concentration of backfill/cover which replaces all pre-remediation concentration that exceed the response goal.

2.7 Contaminant Transport Models

Contaminant transport occurs by advection (bulk movement due to fluid flow), diffusion and adsorption. Deterministic and stochastic approaches have been utilized to model contaminant transport phenomenon. Deterministic approaches include closed form solutions, numerical techniques such as Finite difference and Finite Element Methods. Closed form solutions are always elegant and easy to use. But they are difficult to obtain. Numerical solutions require computational resources and every problem has to be solved

making it time consuming. Since contaminant transport is a function of coordinates in space and time, both analytical and numerical techniques tend to become complex. Deterministic approaches are sometimes considered impractical due to the amount of data required to specify actual heterogeneity of geological materials. In such cases, probabilistic approaches become handy.

A deterministic and macroscopic model for pollutant transport in a heterogeneous medium including diffusion, advection and adsorption was developed by Auriault and Lewandowska (1996). To evaluate the design thickness of earthen barriers, Shackelford (1990) used error functions to solve the traditional transport phenomenon and performed transit-time analyses. Khandelwal and Rabideau (1996) modeled diffusion dominated transport in soil-bentonite slurry walls. Weber and Smith (1987) provided a review of different models available for adsorption processes. Leo and Booker (1996) developed a time-stepping finite element method for analysis of contaminant transport in fractured porous media. Kemblowski and Wijedasa (1995) applied Bayesian analyses for determining contaminant travel time. Ghanem and Dham (1995) performed stochastic characterization of multiphase flow in random porous media. Papers abound in literature that tend to characterize the properties of the geological medium as stochastic variables (Nibori, 1994, Benson, 1991, Bogard, 1990).

2.8 Containment and Capping

For this study, it will be assumed that the site will be peripherally contained by a slurry wall. The top surface will be contained by asphalt cap.

The material in the containment may be subject to forces which could lead to significant changes in material properties over the lifetime of containment facility. For example, long term creep of the compacted soil on the inclined portion of a barrier may tend to alter the permeability of soil. Also, the leachate from buried waste may react chemically with soil, causing changes in microscopic structure and material properties affecting flow. For example, some strong acids, bases organic and inorganic fluids may interact adversely with soil, causing increases in the permeability. (Meegoda and Rajapaske, 1993). Changes in cation valence or electrolyte concentration of soil water caused by permeation with inorganic liquids increase hydraulic conductivity (Anderson 1980, Daniel 1990). According to Anderson et. al. (1980), permeability of soil increases by two orders of magnitude with time upon contact with acetic acid due to the dissolution of soil followed by piping of the particle fragments.

Construction defects in containment and cap may cause structural distress. These defects are a function of quality assurance of construction techniques adopted and materials utilized. Tachavises and Benson (1997) report that permeability increases by several orders of magnitude due to poor construction. They also show that, in such cases, the results approximate the situation with no wall. Giroud and Bonaparte (1989) concluded that 1 defect per 10 meter of seam can be expected for geomembrane liners installed without independent quality assurance. As the thickness of containment decreases over a period of time, efficiencies of the containment and the cap decrease. Efficiency of capping contaminated sediments as a function of cap thickness was computed by Thoma et. al, (1993).

2.9 Flow towards Caps

Liquid contaminants can migrate upward from the soil towards the cap by capillary action. Inorganic contaminants can flow towards the cap by capillary action. The movement of contaminants in capillary zone can be tracked by following equation proposed by Terzaghi,

$$t = n * H_c / k (Ln(H_c /H_c-z) - z/ H_c) \quad (2.6)$$

Where,

t = time required for meniscus of capillary water to rise to the height z above the free water level,

n = porosity,

k = coefficient of permeability,

H_c = height of capillary rise,

z = distance of capillary meniscus from groundwater level.

The height of capillary rise can be calculated by following equation,

$$H_c = C/ e * D_{10}, \text{ cm} \quad (2.7)$$

Where,

H_c is Capillary head, e is void ratio and D_{10} is diameter at 10% passing.

C is a constant varying from 0.1 to 0.5.

Raghu and Hsieh (1988) report that tests conducted in the laboratory indicate that chromium migrates in upward direction in the soil pores upto 5' causing swelling. Due to this, damage to slabs and pavements results.

Flow of volatile contaminants and gases to the cap can be calculated by using air permeability of soil. The flow of air in the continuos air phase form is governed by

concentration or pressure gradient. Both Fick's and Darcy's law can be used to describe the airflow. More details regarding this will be furnished in Chapter 3. According to Corey (1977), the air phase can be treated as continuous as degree of saturation reduces to around 85% or lower.

2.9.1 Flow towards Caps

In order to reach the cap the contaminants have to flow up. In most cases, this flow would be in the capillary zone. Flow towards caps can be modeled by Richard's equation which overcomes the shortcomings of Terzaghi's equation. This equation was employed to model the capillary flow. More details are provided in Chapter 4.

2.9.2 Flow through Caps

It is common practice to provide a layer of stone below the asphalt cap. This layer will enhance the structural integrity of the asphalt pavement as well as act as a capillary break. The gravel layer will also tend to collect the liquid and the gaseous contaminants flowing towards the cap. In such cases, as well as the cases where gas venting is provided in soil, the flow to the cap will be reduced significantly and the flow through the cap may not even has to be considered for Brownfield development.

Flow of chemicals through the cap is a remote possibility. Air permeability of asphalt and concrete is 10^{-6} to 10^{-7} cm/s (Meegoda, 1993). Hence flow of gases through the cap will be insignificant. Cap can crack after sometime. Once this happens, liquids will flow up through the cracks. Organic chemicals can flow up through the cap by volatilization. Under these conditions, flow through cap can be negligible.

CHAPTER 3

DEVELOPMENT OF MODELS FOR FLOW FOR TOWARDS AND THROUGH PERIPHERAL CONTAINMENTS

3.1 Introduction

In this chapter, the following methodologies will be developed sequentially:

a. Contaminant Transport model for flow towards and through the peripheral containment (at the boundary).

b. Determination of cancer risk/ hazard ratio based on exposure and concentration.

For this study, the methodology presented for items above is based on the information presented in a paper by Chirputkar and Raghu (1998).

3.2 Contaminant Transport Model for Flow towards and through the Peripheral Containment

Figure 3.1 portrays the flow chart for contaminant to travel to the face of the peripheral containment/cap and for the flow of contaminant through the peripheral containment/cap.

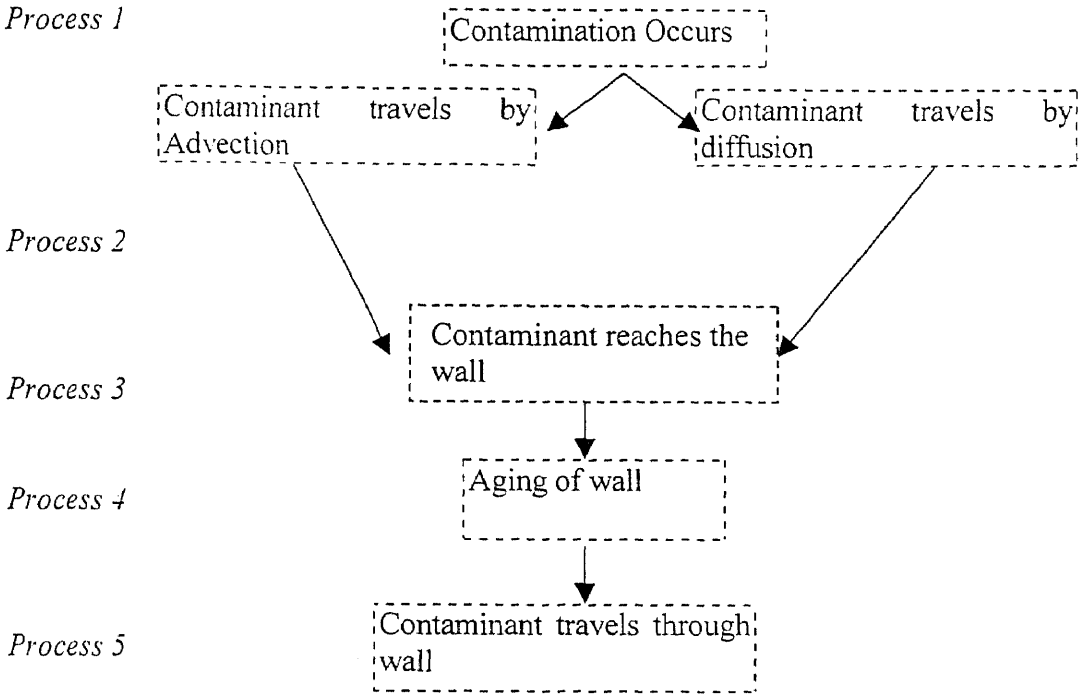

Fig 3.1 Process Tree for contaminant to travel to the face of the wall and for the flow of contaminant through the wall

3.3 Transport Model

The contaminant travels through the soil by advection and diffusion. A process based model can be developed based on the site data. Effects of changes in material properties will be included in the transport model. Adsorption is not considered By neglecting adsorption, contaminant transport model would predict higher flow rate and hence higher risk than actual. This is conservative and hence the assumption is acceptable. Similarly, the risk is predicted conservatively by neglecting degradation. However, in this study the source concentration is indirectly accounted in the source concentration data.

A maximum time period has to be chosen for all calculations involving flows. In this case, this period would be assumed to be 30 years. This is based on the fact that EPA stipulates post remediation monitoring period (post closure) to be 30 years.

3.4 Advection Process

Under this process, bulk movement of contaminant through the soil occurs due to fluid flow. If the contaminant is a volatile contaminant, then it will travel under the pressure head. The flow of contaminant through the soil can be calculated by using equation 3.1. The following equation was derived based on an equation given by Daniel (1990). The details are shown in appendix.

$$C_a(t) = V_s(t) * C(t) * n \qquad (3.1)$$

Where

$C_a(t)$ = contaminant concentration due to advection process which is a function of time.

$V_s(t)$ = Seepage velocity which is a function of time.

C(t) = Source concentration which is a given function of time and

n is porosity.

Based on this data, process function C versus time for use in this study can be obtained. Sample data curves for seepage velocity and concentration are provided in figure 3.2 and 3.3 respectively.

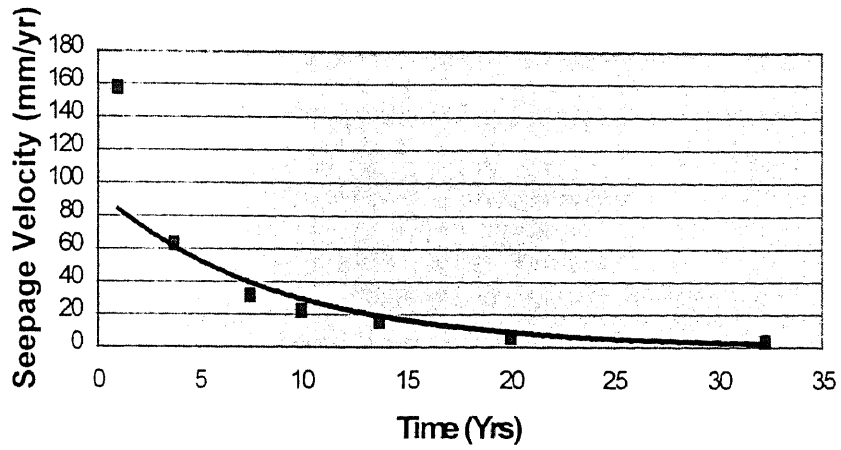

Fig 3.2 Seepage Velocity vs. Time for Cl^-
(Data from Mitchell, 1990)

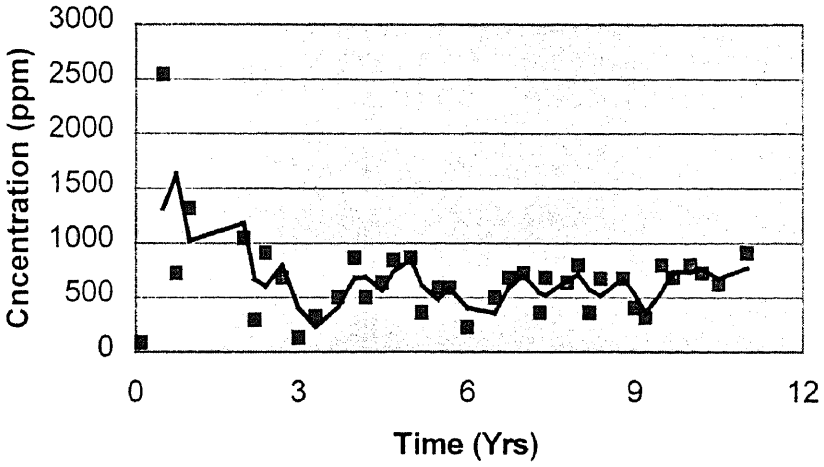

Fig. 3.3 Concentration vs. Time for Cl^-
(After Huebner et. al., 1995)

3.4.1 Point Sources vs. Concentration Contours

In previous section, the contamination is assumed to originate from a point source. In order to utilize the point source model, field data in form of concentration contours has to be converted to equivalent point sources. This can be accomplished in following manner.

$$C = \Sigma(A_i C_i)/. \Sigma A_i \quad (3.2)$$

Where,

C is equivalent source contaminant concentration.

A_i and C_i are respectively area and concentration of a subarea within a contour.

The locations of the sources are calculated by following formulae,

$$X = \Sigma(A_i C_i) Xi/\Sigma(A_i C_i) \quad (3.3)$$

$$Y = \Sigma(A_i C_i) Y_i/\Sigma(A_i C_i) \quad (3.4)$$

Where X_i and Y_i are respectively the coordinates of the center of gravity of a subarea within a concentration contour and X and Y are respectively the coordinates of the center of the gravity of the concentration contour.

3.4.2 Multiple Point Sources

There can be multiple point sources at a given site. Concentration contours can be converted to multiple point sources as shown in section 3.4.1.

3.4.3 Travel Time from Source to Wall

The contaminant will travel from different sources to the wall and reach different locations of the wall at different times. It will be assumed conservatively that contaminants from different sources will arrive at the same location of the wall. But they

will arrive during different times. Hence it will be necessary to calculate the travel times of the contaminant from different sources to the wall to obtain the total quantity of contaminant at the wall from different sources as a function of time.

Distance traveled $= {}_0f^t \; V_s(t)\, dt$ (3.5)

Seepage velocity V_s can be expressed as,

$V_s = V_o * e^{-\alpha t}$ (3.6)

Substituting for $V_s(t)$ from equation (5), and integrating

$$d = V_o(1 - e^{-\alpha t}) / \alpha \quad (3.7)$$

d = Distance traveled.

3.5 Diffusion Process

Only chemical diffusion process has been considered. Changes in the contaminant gradient vs. time have been shown in Figures 3.6 and 3.7.

The concentration of a contaminant by diffusion can be calculated using equation

$C_d(t) = G(t) * D^* * n(t)$ (3.8)

Where,

G(t) = Chemical gradient of a contaminant which is a function of time.

$= (\delta C/\delta x)(t)$

$C_d(t)$ = Concentration of a contaminant in diffusion process which is a function of time.

C(t) = concentration of a contaminant which is a function of a time.

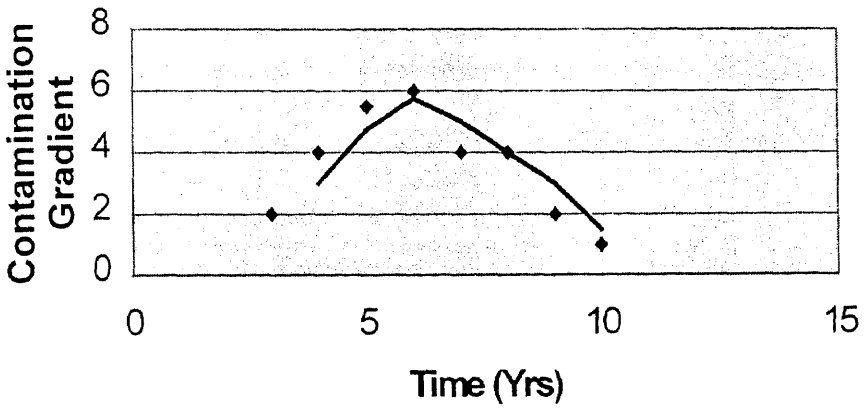

Fig. 3.4 G vs. Time
(Calculated from data provided by Anderson)

$\delta C/\delta x$ values for two different sites were computed based on the available data.

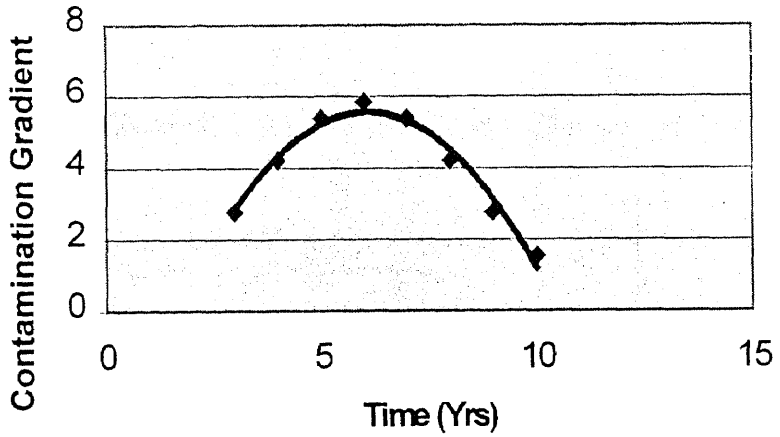

Fig. 3.5 G(t) vs. Time
(Calculated from data provided by Anderson)

Based on above Figures 3.6 and 3.7, $\delta C/\delta x$ vs. time data for use in this study, can be obtained.

3.6 Determination of Concentrations at the Outer Face of the Wall

The concentrations at the outer face of the wall are influenced, in addition to the quality of construction of the wall, by the concentrations at the inner face of the wall and the dimensions of the wall. For this study, two different scenarios will be analyzed. One will be for the condition corresponding to the wall built with good quality of construction and 100% structural integrity of the wall (no aging). The other case will represent walls constructed with poor quality of construction and structural integrity of the wall impaired by aging. Also, the contaminant coming out of the wall may accumulate if there is a marsh like soil condition. On the other hand, the contaminant will drain away if there are favorable soil conditions on the outside of the wall. Each of the above two cases are analyzed for the two scenarios presented above. These four conditions represent the best and the worst possible situations.

For good construction,

Thickness Fraction T = 1, for 0=< time =< 20 years

Thickness Fraction T = (1- (59/60) x (t-20) t>20 years (3.9)

Thickness fraction is the ratio of thickness at a given time to the initial thickness.

For poor construction, the wall function is assumed as follows,

Thickness Fraction T = 1 for 0=< time =<5 years

Thickness of wall T = (1-(0.033 x (t-5)) t>5 years (3.10)

Equations 3.7 and 3.8 are based on the assumption and data in literature that a wall built with good construction practices will deteriorate after a period of 20 years. Whereas a wall built with poor construction practices is assumed to deteriorate after a

period of 5 years. These values as a functions of time are called Wall functions and are shown in Figure 3.8 below

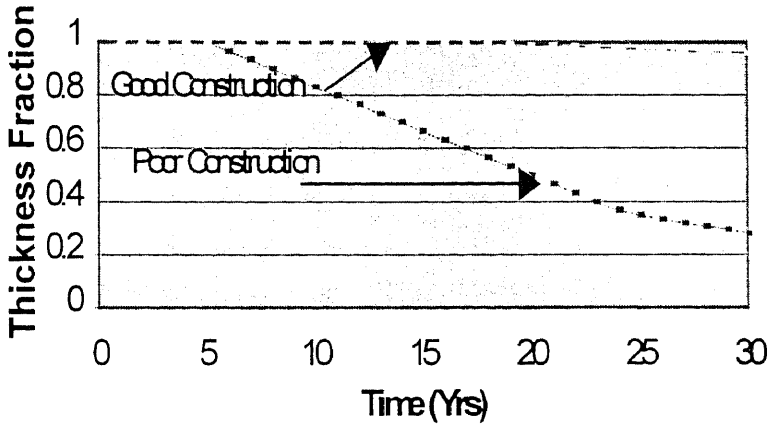

Fig. 3.6 Wall Functions

The concentrations at the outer face of the wall taking advection and diffusion into account can be calculated using following equation,

$$C_o(t) = (C_i(t)*h(t))\,(V_s*n(t) + n(t) * D^*) / (h(t) + n(t) * D^*) \qquad (3.11)$$

Where,

$C_o(t)$ = Concentration of a contaminant on outside face of a slurry wall as a function of time.

$C_i(t)$ = Concentration of a contaminant on inside face of a slurry wall as a function of time.

$V_s(t)$ = Seepage Velocity as a function of time and

$n(t)$ = Porosity of the wall expressed as function of time.

$$= ((T(t)\,(1+e_0))-1)/(T(t)\,(1+e_0)) \qquad (3.12)$$

Where,

h(t), e(t). n(t) and T(t) are respectively thickness. void ratio, porosity, and wall function at any time t and e_0 is the initial void ratio of the slurry wall.

Derivation for equation 3.11 and 3.12 are presented in Appendix B.

Cumulative concentrations will indicate the effects of accumulation of contaminant at the outside of the containment. Concentrations for the four different scenarios considered for each contaminant can thus be determined.

3.7 Determination of Risk/Hazard Ratio

The relevant contaminant concentrations will be input to a CalTOX model. Risk/hazard ratio will be the output from the model. Details of these calculations for applications will be explained in Chapter 5. For each contaminant, risk and/or hazard ratio vs. time plot will be obtained. An attempt will be made to quantify the total absolute risk/hazard ratio for the site. It is possible to utilize this process for different treatment/containment scenarios. Results obtained can be used as a decision making tool for the development of Brownfield Sites.

CHAPTER 4

DEVELOPMENT OF MODEL FOR SURFACE CONTAINMENTS

4.1 Introduction

In this chapter, the following methodologies will be developed sequentially:

a. Contaminant Transport model for flow towards and through the upper surface containment.

b. Determination of cancer risk/ hazard ratio.

4.2 Contaminant Transport Model for Flow towards and through the Surface Containments

Figure 4.1 portrays the process tree for contaminant to travel to the face of the cap and for the flow of contaminant through the cap.

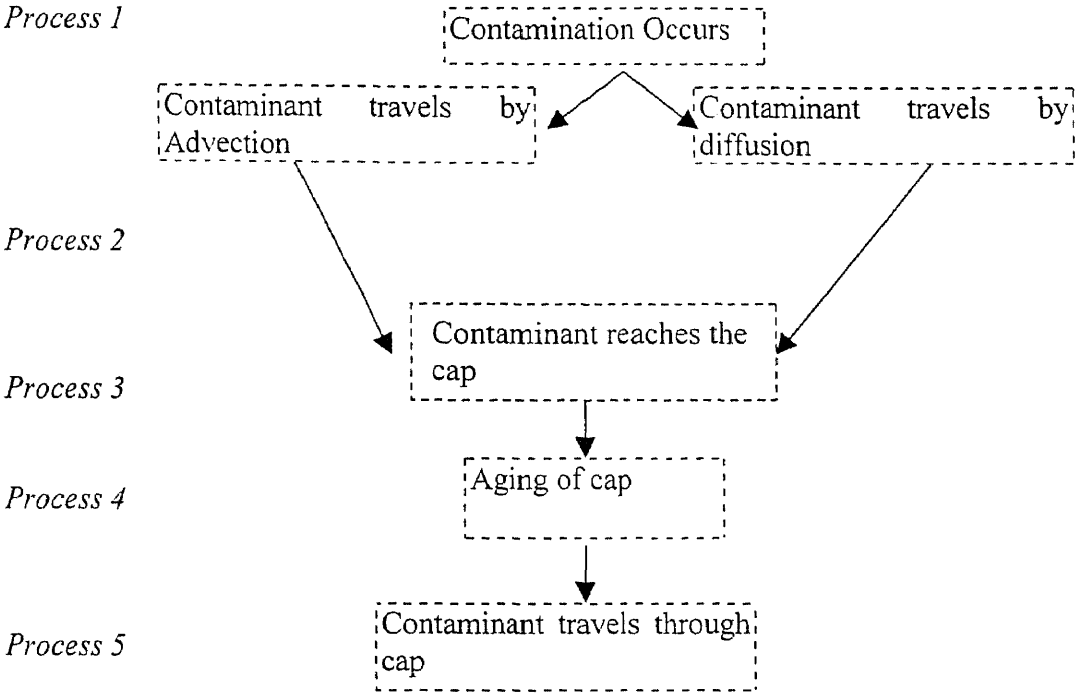

Fig 4.1 Process Tree for contaminant to travel to the face of the wall and for the flow of contaminant through the cap.

4.3 Flow of Contaminants in Capillary Zone

The concept of capillary action and surface tension are widely known. These principles have been applied to a satisfactory extent to represent the movement of liquids in unsaturated zone in upward direction.

If a soil in the state of a dry powder is brought into contact with water, the water will at once tend to be drawn into the voids by capillary action. The velocity with which the water is absorbed into the soil is dependent on the pore size of the soil. As the height increases, the degree of saturation decreases considerably. Finally, there is a limiting value above which water can not be drawn.

4.4 Richard's Equation

Richard's Equation overcomes most of the limitations of Terzaghi's equation. It is derived by the concept of mass conservation. This equation contains various terms for moisture contents, soil suction, and permeability as variable. The moisture content in Richard's equation is expressed as a volumetric moisture content. However, this moisture content is related a gravimetric moisture content. The gravimetric moisture content can be easily measured in the laboratory. Moisture content and soil suction are related to each other by a curve known as soil suction curve.

Richard's equation can be used to describe the flow in unsaturated soils. The equation has been extensively used to model infiltration. However, the same equation has not been solved to model the capillary flow.

As discussed in Chapter 2 earlier, liquid and gaseous contaminants from the soil flow up towards the cap. Flow of liquids in the vadose zone can be modeled by Richard's equation. (Jury, Gardener and Gardener 1991). This equation, presented below, relates water fluxes, storage changes, and sources and sinks of water.

$$\partial\theta/\partial t = \partial/\partial z(K(h)\,(\partial h/\partial z + 1)) \qquad (4.1)$$

Where,

θ is the volumetric water content, h is the matrix suction and z is the vertical dimension respectively. The volumetric water content, θ is defined as ratio of volume of water to volume of solids.

Equation 4.1 can not be solved in the form it is in, because it contains two unknowns θ and h and only one equation. This difficulty may be overcome by expressing it in either water characteristic or matric potential form.

The water content form of Richard's Equation is as follows:

$$\partial\theta/\partial t = \partial/\partial z \left(D_w(\theta)\, \partial\theta/\partial z\right) + \partial K(\theta)/\partial z \qquad (4.2)$$

Where,

$D_w(\theta)$ = Soil Water Diffusivity

$= K(\theta)\, dh/d\theta$

$K(\theta)$ = Permeability of soil as a function of water content.

Solution of the equation 4.2 will yield θ, the water content, as a function of "z" and "t". Knowing the water content, the concentration of a contaminant per liter can be determined.

The matric potential form of Richard's equation is as follows,

$$C_w(h)\, \partial h/\partial t = \partial/\partial z((K(h)\, (\partial h/\partial z + 1)) \qquad (4.3)$$

Where,

$C_w(h)$ = Water capacity function

$K(h)$ = Permeability of soil expressed as a function of matric potential.

4.5 Solution of Richard's Equation

There are three types of partial differential equations, elliptic, parabolic and hyperbolic differential equations.

Any partial differential equation can be represented by Equation 4.4.

$$Au_{xx} + 2Bu_{yx} + Cu_{yy} + Du_x + Eu_y + Fu + G = 0 \qquad (4.4)$$

u_{xx} = Second Order Partial Derivative of a Function u with respect to x

u_{yy} = Second Order Partial Derivative of a Function u with respect to y

u_{xy} = Second Order Partial Derivative of a Function u with respect to x and y

u_x = First Order Partial Derivative of a Function u with respect to x

u_y = First Order Partial Derivative of a Function u with respect to y

A, B, C, D, E and F are constants.

The partial differential equation can be classified using the discriminant as shown below:

Discriminant $d = AC - B^2$ (4.5)

Table 4.1 classifies the partial differential equation on discriminant (Gustafson, 1976)

Table 4.1 Types of Partial Differential Equations

Discriminant	Equation Type
$d > 0$	elliptic
$d = 0$	parabolic
$d < 0$	hyperbolic

Based on the above table, Richard's equation is parabolic a partial differential equation and is of the nonlinear second order type. The equation itself does not have any expression for maximum value of capillary rise. Hence the maximum capillary rise, calculated from expression containing particle size, was imposed as boundary condition.

Analytical solutions can not be obtained for nonlinear partial differential equation such as Richard's equation. Hence numerical methods have to be looked at. Solution of partial differential equation can be obtained by various numerical methods such as finite

element method, finite difference method. The difficulty with Richard's equation is that it does not fit into any standard form of equation such as heat equation, wave equation or Laplace's equation. A brief review of prior work done involving solution of Richard's equation by numerical techniques will be provided.

4.5.1 Prior Work Done in Solving Richard's Equation

Lim and Lee (1993) used Galarkin Method to solve the problem of one dimensional, vertical flow of water and mass transport of reactive and nonreactive solutes in unsaturated porous media. Numerical approximations based on different forms of governing differential equation can result in remarkably different solutions although they are equivalent in continuos forms.

Van Dijke and Van Zee (1995) used Richard's equation for air injection into groundwater in a homogeneous axially symmetric porous medium. A numerical method based on mixed form of Richard's equation was obtained. However, the results they obtained were compared with those for steady state solutions.

Lam and Barbour (1979) et. al. presented a saturated-unsaturated finite element model to simulate the movement and distribution of the contaminants in groundwater flow systems. The finite element solution was obtained by using Galarkin weighted residual method. The nonlinear equation was solved using iterative techniques. However, the drawback was that material properties were assumed as constant.

Tim and Mostagini (1989) presented a finite element model based on Galarkin's weighted residual technique to predict the advective-dispersive transport and

transformation of pesticides and metabolites in the unsaturated zone. However, material properties were assumed as constant.

Energy methods are not suited very well for solving time dependent problems. For instance, most dynamics problems utilize finite difference technique for time dependence. This may be due to problems in developing variational formulations based on energy for nonlinear time dependent equations. Hence finite difference methods were employed for this study.

The functional relationship between suction, water content and permeability allows one to handle nonlinearity in equation elegantly by utilizing finite difference technique.

4.5.2 Formulation of Richard's Equation

The final form of formulation of Richard's equation is given in equation 4.6. Detailed derivation is given in Appendix C.

$$\theta(I+1,J) = (KH\Delta t/\Delta z^2)\,(\mathbf{k}(I,J+1)\,\mathbf{h}(I,J+2) - \mathbf{k}(I,J+1)\,\mathbf{h}(I,J+1) - \mathbf{k}(I,J)\,\mathbf{h}(I,J+1) + \mathbf{k}(I,J)\,\mathbf{h}(I,J) + \Delta \mathbf{z}\,(\mathbf{k}(I,J+1) - \mathbf{k}(I,J))) + \theta(I,J) \quad (4.6)$$

$$\theta(I+1,J) = (KH\Delta t/\Delta z^2)\,(\mathbf{k}(I,J+1)\,\mathbf{h}(I,J+2) - \mathbf{k}(I,J+1)\,\mathbf{h}(I,J+1) - \mathbf{k}(I,J)\,\mathbf{h}(I,J+1) + \mathbf{k}(I,J)\,\mathbf{h}(I,J)) + (K\Delta t/\Delta z)\,((\mathbf{k}(I,J+1) - \mathbf{k}(I,J))) + \theta(I,J) \quad (4.7)$$

$$(K\Delta t/\Delta z) = (KH\Delta t/\Delta z^2) * (\Delta z/H) \quad (4.8)$$

I = Time Coordinate

J = Spatial Coordinate

θ = Water Content

k = Normalized Permeability i.e. a ratio of permeability at a given water content to maximum value of permeability, which is saturated permeability.

h = Normalized Matric Suction i.e. a ratio of matric suction at a given water content to maximum value of matric suction

Δz = Normalized increment in space i.e. a ratio of increment in space to maximum capillary rise.

K = Maximum value of permeability

H = Maximum value of Matric Suction

Δt = Time increment

Δz = Space increment

$(KH\Delta t/\Delta z^2)$ is called as diffusivity and is a dimensionless constant. $(K\Delta t/\Delta z)$ is called as permeability grid constant and is also a dimensionless constant.

4.5.3 Choice of Time Step

The choice of time step Δt is important. If Δt is too large, the solution may not converge in case of explicit differential equation formulation. In case of implicit differential equations, the iteration process may converge for nonlinear problems. On the other hand, if the time step is too small, extra effort may be required.

For Euler forward explicit time integration scheme, it is recommended that the value of dimensionless fourier number $(KH\Delta t/\Delta z^2)$ should be less than 0.25 (Adina Ref. Manual, 1995).

Where,

K = Saturated Permeability

H = Maximum Suction

Δt = time step

z = vertical grid spacing.

4.5.4 Determination of Soil Parameters

There are two versions of the program to determine the soil parameters. In the first version of the program, the soil suction and permeability are expressed as functions of the water content. Each value is calculated from a curve fitting expression. The second version of the program takes the raw laboratory data for soil suction and unsaturated permeability and calculates water content using numerical interpolation.

4.5.5 Finite Difference Schemes

Two numerical schemes, forward difference scheme and predictor corrector scheme were employed for solution of Richard's equation. Details of the implementation of the model are given in chapter 6.

4.5.5.1 Forward Difference Scheme: In this method, the derivatives at any node are computed from the values at the node and at the forward node. Utilizing these values, volumetric water content at the next time step is calculated from those at the previous time step.

4.5.5.2 Predictor Corrector Method: In this method, at first the volumetric water contents are computed based on forward difference technique. Then, the derivatives of the various functions are computed for the average value of the water content between

time step were computed again from the previous step. These values were compared with the previously determined values. If the differences between these values are greater than 1%. this process of calculation is continued until the required accuracy is obtained.

4.6 Calculation of Contaminant Concentration

The contaminant concentration will be calculated by following equation

$C = (\theta_f - \theta_i)$ * Dissolved Concentration in groundwater (4.9)

Where,

C = Contaminant Concentration at surface

θ_f = Final water content

θ_i = Initial water content.

Concentration of contaminant in dissolved groundwater is obtained from field data.

4.7 Installation of a Gravel Bed

It is well known that a gravel layer under any pavement would tend to distribute the loads and to minimize the extent of cracking of the course. In our study, the gravel layer would also the following additional functions,

1. It would serve as a collector for volatiles in case if venting system is used.
2. This gravel layer can also function as a drain for the contaminants flowing towards the top in the vadoze zone. The impact of this layer on risk and development on Brownfield site will be discussed in Chapter 6.

4.8 Determination of Risk/Hazard Ratio

The contaminant concentration calculated by equation no. 4.9 will be provided to CalTOX model and risk/hazard ratio will be calculated as discussed.

4.8.1 Determination of Risk Due to Chromium Contamination

CalTOX model in the present form can not determine risk due to hexavalent chromium . So this model was modified. For this purpose, a modified fugacity approach for inorganic chemicals (Mackay and Diamond, 1989) was utilized. Properties required were obtained from literature from literature (Lehman A., 1979, Diamond and Lamprecht, 1996). For the determination of acceptable risk, data regarding contaminants as a function of time shown in figure 4.2 is utilized. Risk vs. time data generated from the above data is shown in figure 4.3. Some details of this approach are presented in Appendix D. According to this method, a hexavalent chromium concentration of 26 ppm is acceptable and concentration above this limit causes cancer. The corresponding allowable concentration according to EPA is 10 ppm.

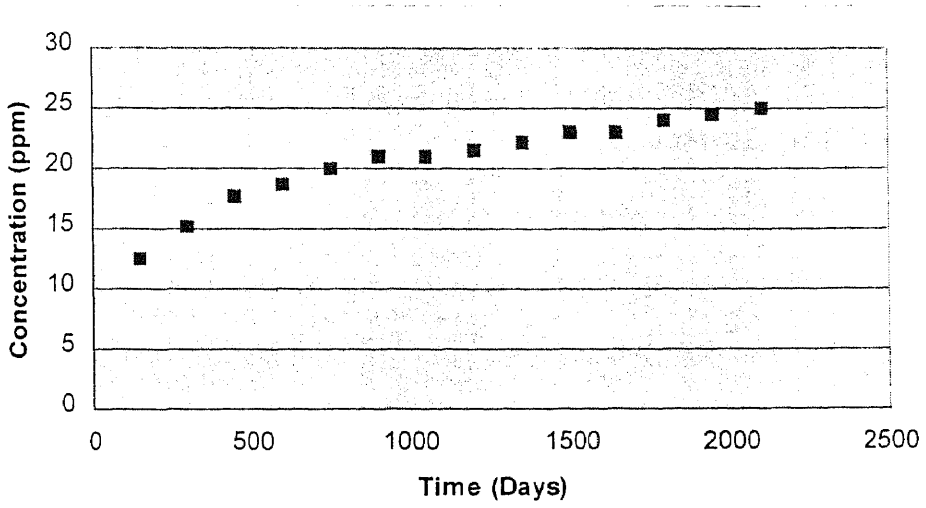

Fig 4.2 Concentration of Contaminant (Cr^{+6}) at Inner Surface of Surface Containment vs. Time

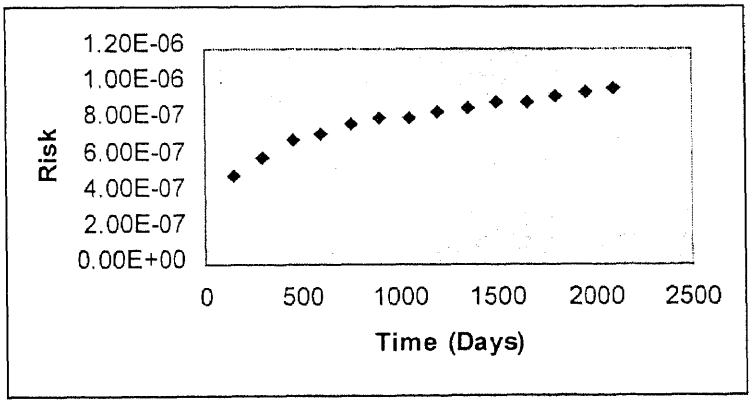

Fig. 4.3 Risk vs. Time at Inner Surface of Surface Containment vs. Time for Cr^{+6}

CHAPTER 5

RESULTS AND DISCUSSIONS FOR FLOW TOWARDS AND THROUGH PERIPHERAL CONTAINMENTS

5.1 Introduction

In this chapter, three case studies were analyzed by the model proposed. In case study No. 1, anthracene was the main contaminant from a single source. In case study, No. 2 trichloroehylene (TCE) with multiple sources was the dominant contaminant. In case study No. 3, benzene, was the targeted contaminant determined from contamination contours.

5.2 Case Study No. 1

5.2.1 Site Description

The site chosen for this study is in Northern New Jersey and has an area of nine acres. It slopes towards and is located adjacent to a river as shown in Figure 5.1. A small jetty connects the site and the river. The site was closed in 1988 down due to contamination. A preliminary investigation of the site was performed in 1991. This was followed by a remedial investigation in 1996.

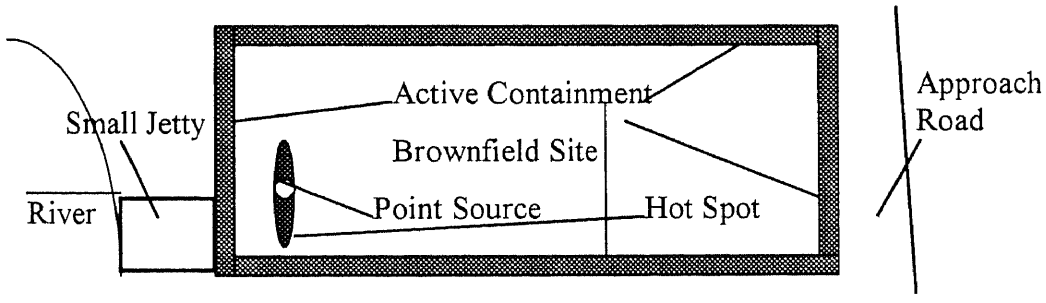

Fig. 5.1 Schematic Diagram of Site

Later on, a developer showed an interest to build an industrial warehouse on this site, as it was located in an industrial area. The developer proposed to install a thick asphalt cap with a gravel bed under the cap as a capillary break. Surface soil samples were collected with decontaminated stainless steel spoons. Fill materials consisting of silty clay were observed in of the surface soil samples collected in preliminary investigation and remedial investigations. A layer of stiff red clay occurred at approximately 10 feet below the ground level and bedrock was encountered at 20 feet below ground level. Ground water was observed at 3 to 4 feet below ground surface and pH of the ground water was found to be between 4 to 4.5. The main contaminant at the site is toluene.

The contaminant is mostly concentrated in a corner of the building and thus it has been modeled as a point source as shown in Figure 5.1. A bentonite slurry wall extending to bedrock is proposed to be installed in this site to prevent flow of contaminant to the river. In this study, the movement of anthracene through the slurry wall is modeled and the risk due to the movement of contaminant is determined. Due to the proposed provision of a capillary break under the cap and due to the fact that capillary water was not observed, the risk due to contaminant flowing to and through the cap was not modeled. The transport model for flow to and through the slurry wall is presented below.

5.2.2 Seepage Velocity

Fig 5.2 is the plot of. V_s as a function of time obtained from site data. can be represented as in Equation below:

$$V_s(t) = V_o * e^{(-\alpha * t)} \quad (5.1)$$

Where,

$V_s(t)$ = Seepage velocity at a given instant of time,

V_o = Initial velocity of the contaminant and

α = A parameter obtained by curve fitting.

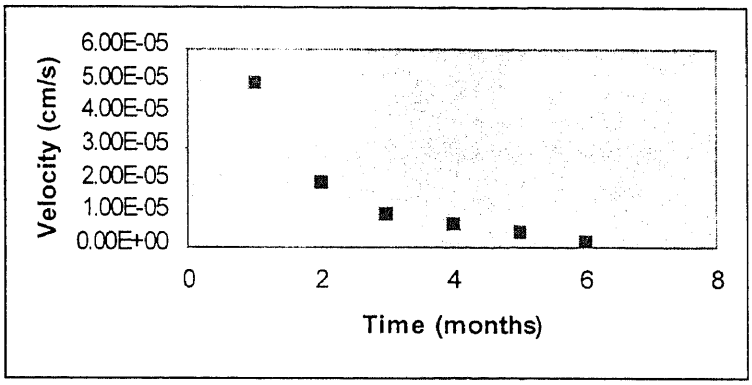

Fig. 5.2 Seepage Velocity vs. Time Considered for this Study

5.2.3 Source Concentration

Concentration versus time, a process a function, is determined from the site concentration contours and can be represented as:

$$C(t) = C_o * e^{(-\beta * t)} \quad (5.2)$$

Where,

C(t) = Concentration of a contaminant at a given instant of time,

C_o = Initial concentration of contaminant, taken as a single source from site data

β = A parameter obtained by curve fitting.

The source concentration vs. time data was obtained from site data utilized for our study is shown in Figure 5.3.

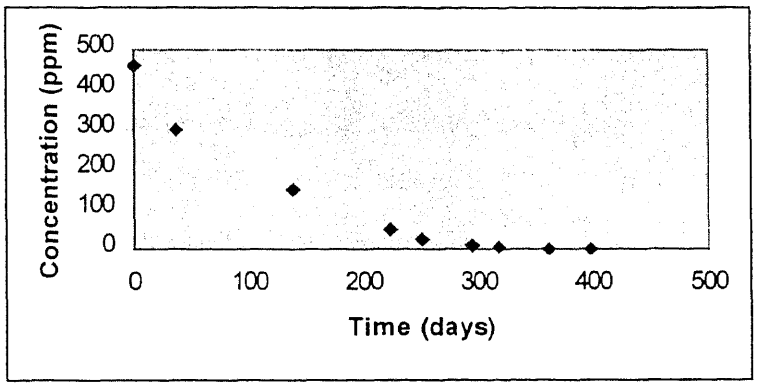

Fig. 5.3 Concentration vs. time considered for this Study

5.2.4 Chemical Gradient

Based on the Figures 3.2 and 3.3, chemical gradient is represented by the following equation,

$$G(t) = (E/ B) * e^{-D} \qquad (5.3)$$

Where,

E = $G_{max.}$ = Maximum value of contaminant gradient at a given location from a given source,

B = $(2 * \pi)^{1/2} * t_{\sigma}$

D = $(E /2) * ((t - t_{\mu})/t_{\sigma})$,

t_{μ} = Mean time of contaminant travel and

t_σ = Standard deviation of contaminant travel time.

t = Time at any given instant.

The plot in Figure 5.4 shows the chemical gradient data used for this study, obtained from figure 3.4 and 3.5.

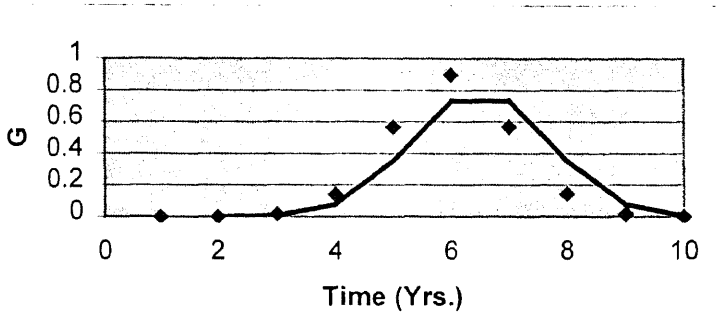

Fig. 5.4 Chemical Gradient vs. Time Plot Utilized for Present Study

5.2.5 Determination of Concentration at Inner Face of Wall

All the above processes, such as advection and diffusion, are considered as independent processes. Hence the concentration inside the face of the wall is given by:

Concentration at the inner face of the wall = Eqn.5.1 * Eqn.5.2 + Eqn.5.2* Eqn.5.3 (5.4)

Values of concentration at the inner face of the wall were computed and are presented in figure no. 5.5.

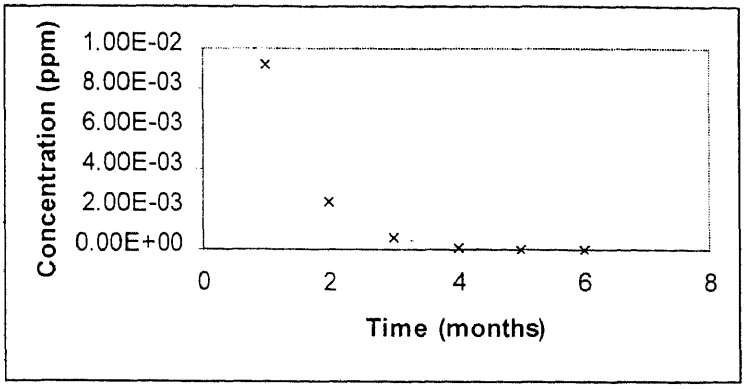

Fig 5.5 Contaminant Concentration at the Inner Surface of Containment vs. Time

5.2.6 Determination of Concentrations at the Outer Face of the Wall

For computing output concentrations from equation 3.13, initial thickness (h_o) of wall has been taken to be 600 mm. The thickness fraction T(t) values were obtained from equation 3.11 and 3.12. For the wall, diffusion coefficient D^* equal to 10^{-9} m^2/sec was considered (Shackleford, 1990). For the ranges of interest in this study, values of n, computed from equation 3.14, varied from 0.84 to 0.95. Therefore a constant value of 0.95 was used.

In order to estimate the seepage velocity through the wall, the following procedure was adopted. It was assumed that the permeability of the wall was about 5 orders of magnitude less than that of soil. The permeability of the wall increases by 4 orders of magnitude upon cracking. (Tachavises and Benson 1997) Hence the permeability of the wall after cracking was taken to be one order of magnitude less than that of the soil. Since the seepage velocity is proportional to the permeability, the seepage velocity through the wall was taken as 1/10 of that through the soil.

The output concentrations for the four scenarios discussed previously are presented below in Figures 5.6 and 5.7 respectively. The concentration vs. time data was input to the CalTOX model and risk, in terms of hazard indices, were determined and

presented in Figures 5.8 and 5.9 respectively. To assess the overall potential for non-carcinogenic effects posed by more than one chemical a hazard index approach has been developed based on EPA's "Guidelines for Health Risk Assessment of Chemical Mixtures". Maximum permissible value for Hazard Index is 1.

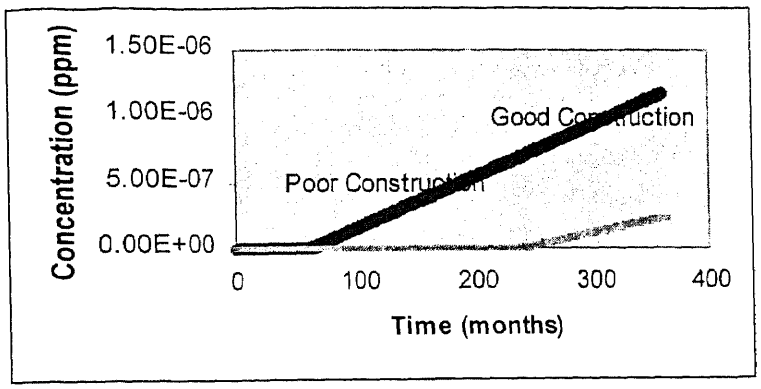

Fig. 5.6 Concentration of Contaminant, Carried Away from Face of Wall (High Permeability Soil)

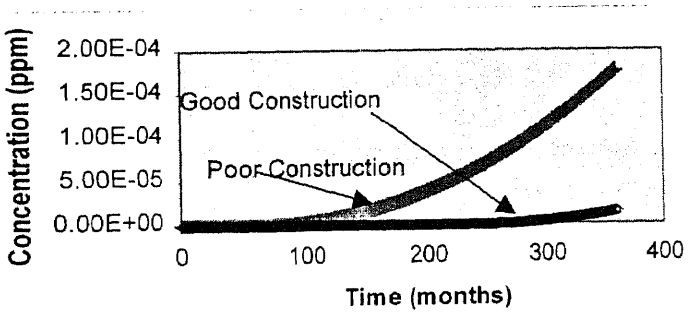

Fig.5.7 Concentration of Contaminant, Accumulating at Outer Face of Wall (Low Permeability Soil)

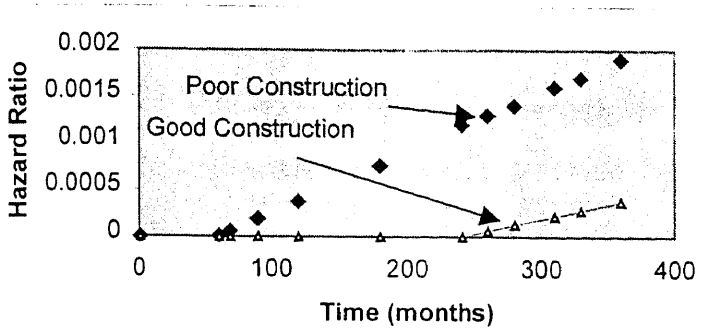

Fig. 5.8 Hazard Index at Outer Face of Wall, Contaminant Carried Away from Face of Wall (High Permeability Soil)

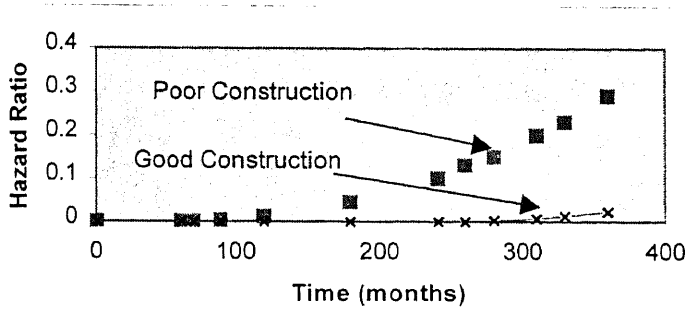

Fig. 5.9 Hazard Index at Outer Face of Wall, Contaminant Accumulating at Outer Face of Wall (Low Permeability Soil)

Comparing Figures 5.5, 5.6 and 5.7, the concentrations at the inner surface of the wall and those at the outer surface of the wall due to poor construction follow a normal trend. It is to be noted that in the latter case, the concentrations are only one half of those in the former case. This illustrates that, in a poorly constructed wall even with drainage or a high permeability soil on the outside, significant leachate of contaminant occurs. This coupled with information in figure 5.8, points out the importance of drainage outside the wall. Thus, it is advisable to have a leachate collection system outside the wall, especially if the quality of construction is poor and the soil outside the wall is of low permeability.

5.2.7 Determination of Risk/Hazard Index

Figures 5.8 and 5.9 show the risk in terms of hazard index for the four scenarios discussed in this paper. The trend of risk seems to follow the trend of the concentrations at the outer surface of the wall. For all the scenarios analyzed the risk is below 1 and hence it is acceptable. If it is not, suitable measures such as pretreatment of contaminant in the site and/or proper disposal of leachate collected at the outside of the wall may be needed.

5.3 Case Study No. 2

5.3.1 Site Description

The site under study is located in a highly industrialized area in Northern New Jersey. The top 15 feet is underlain with fill materials consisting of silty sand. Below the fill is a layer of red silty clay about 10 feet thick. The bedrock, which is the Newark Formation of the New Brunswick Shale, underlies the clay. Water table was at a level of 8 feet below the ground surface.

Figure 5.10 represents a schematic location of the site considered for this study. Trichloroethylene (TCE) was detected in the fill at 4 borehole locations that were utilized for sampling. The initial concentrations in the locations 1, 2, 3 and 4 were respectively 11,000 ppm, 14,000 ppm, 11,000 ppm and 11,000 ppm respectively. These pollutants were generally at a depth of about of 8 feet below the ground surface. These locations have been treated as point sources of contamination. Flow of pollutants has been assumed to occur through the groundwater in the fill through the silty sand layer. Because of this,

advection is considered to be the prominent phenomena. Flow due to capillary action is, not considered since the soil at site consisted of sand.

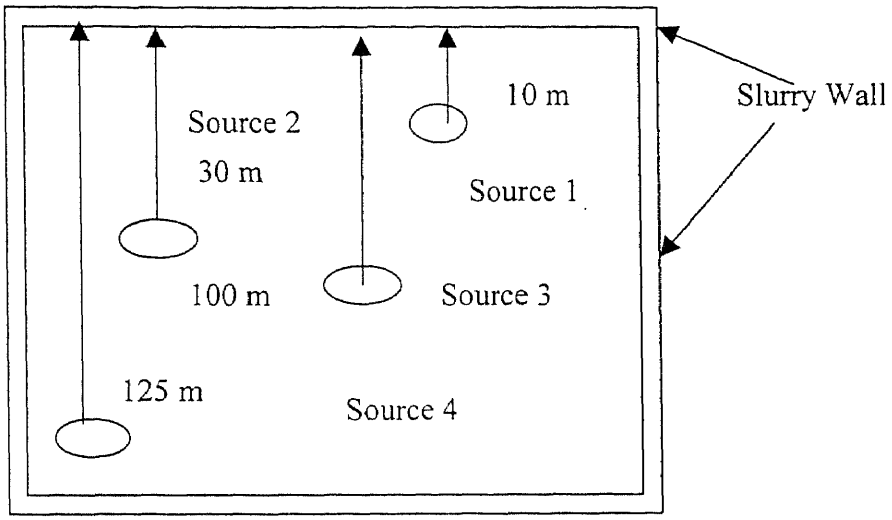

Fig. 5.10 Schematic Representation of Site

5.3.2 Seepage Velocity

The input data for V_s adopted for this study is shown in Figure 5.11.

Since the conditions were similar, for this study, the seepage velocity V_s, of TCE to be used is shown in Figure 5.11 below (Barry et. al., 1997).

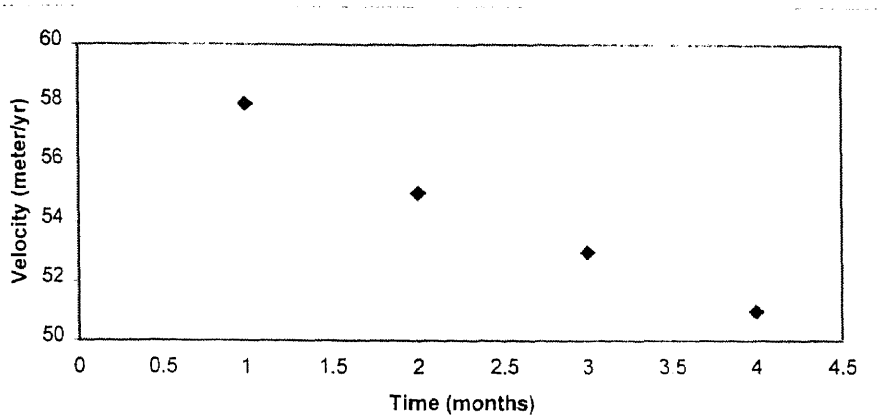

Fig 5.11 Seepage Velocity vs. Time
(After Barry et. al., 1997)

Based on the above data, the seepage velocity, which is a process function, can be represented as in Equation 5.4 below.

$$V_s(t) = V_o * e^{(-\alpha * t)} \qquad (5.4)$$

Where,

$V_s(t)$ = Seepage velocity at a given instant of time,

V_o = Initial velocity of the contaminant and

α = A parameter obtained by curve fitting.

= 5.40×10^{-4} for the data in Figure 5.11.

5.3.3 Source Concentrations

Source concentration versus time, a process a function, is shown in Figure 5.12 for the sources 1, 2, 3 and 4. The variation of concentratrion with time was determined based on interpolation of available data.

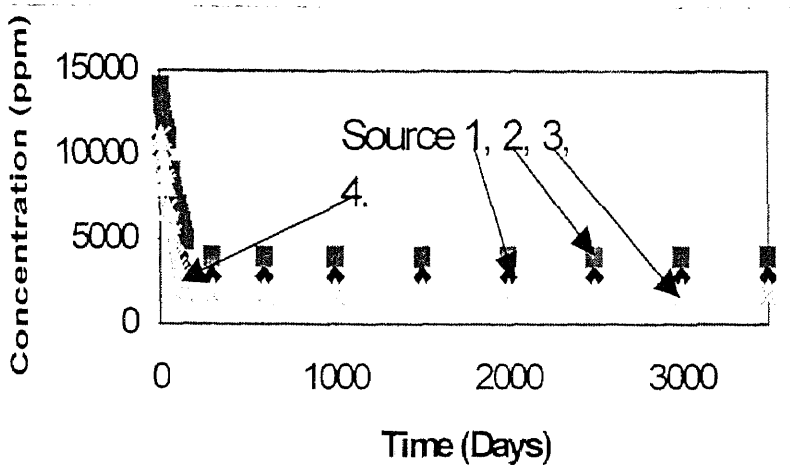

Fig. 5.12 Concentration vs. Time for TCE source 1. 2. 3 and 4.

5.3.4 Contaminant Concentration at Inner Surface

Time required t to travel a given distance d from a source can be calculated from equation 3.6. Travel times from sources 1, 2, 3 and 4 have been determined to be respectively 65 days, 200 days, 769 days, and 1000 days. In other words, the quantity of contamination reaching the wall will be due to source 1 from 65 to 200 days and will be due to sources 1 and 2 from 200 days to 769 days. Flow due to sources 1, 2 and 3 reaching the wall will be from 769 to 2000 days and flow due to sources 1, 2, 3 and 4 reaching the wall will be after 2000 days. This has been computed and shown in Figure 5.13. Spikes are observed corresponding to 200, 769 and 1000 days respectively in the Figure 5.13 below due to flows reaching the wall from sources 2, 3 and 4.

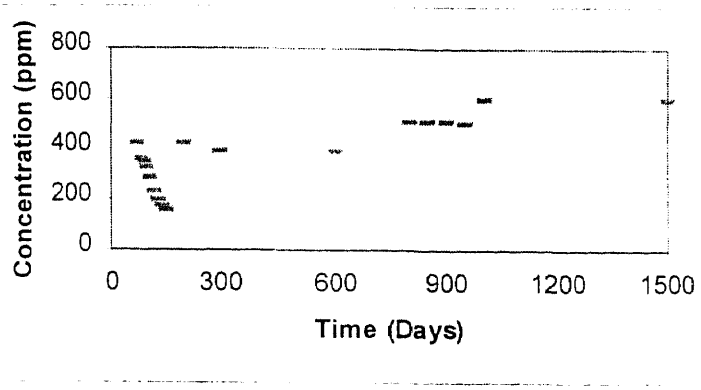

Fig. 5.13 Contaminant Concentration at Inner Face of Wall

5.3.5 Determination of Contaminant Concentration at Outer Surface for Multiple Point Sources

This is determined from equation No. 3.13. The diffusion data utilized was the same as that shown in Figure 5.4.

Of the four scenarios considered for case history no.1, the following two are analyzed,

1. Poor Construction with contaminant carried away from the outer face of the wall.
2. Poor Construction with contaminant accumulating at the outer face of the wall.

The above two are considered as worst cases scenarios. Figures 5.14 and 5.15 show the results for the above two cases. For computing output concentrations, h_o has been taken to be 600 mm. The thickness fraction T(t) values were obtained from equation 3.12. A diffusion coefficient D^* equal to 10^{-9} m^2/sec. was considered. For the ranges of interest in this study, values of n, computed from equation 3.14, varied from 0.84 to 0.95.

Comparing Figures 5.14 and 5.15, it is observed that the source concentration as well as the concentration at the inner surface of the wall exhibit an exponentially decreasing trend with time. In fact, it appears that the inside concentration at any time is about 1/200 times the source concentration. The reduction factor of 1/200 can be attributed to the very low initial seepage velocity of about 60 mm/year.

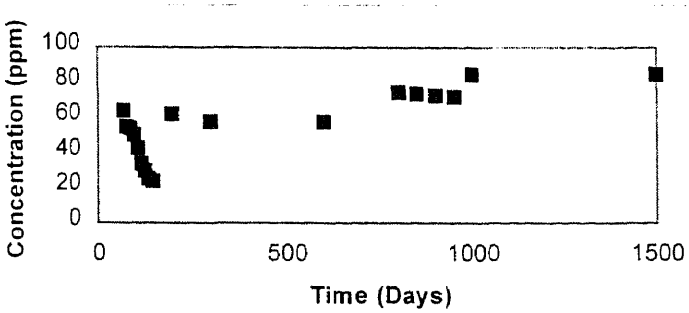

Fig. 5.14 Contaminant with Multiple Point Sources Carried Away from the Face of the Wall (High Permeability Soil) with Poor Construction.

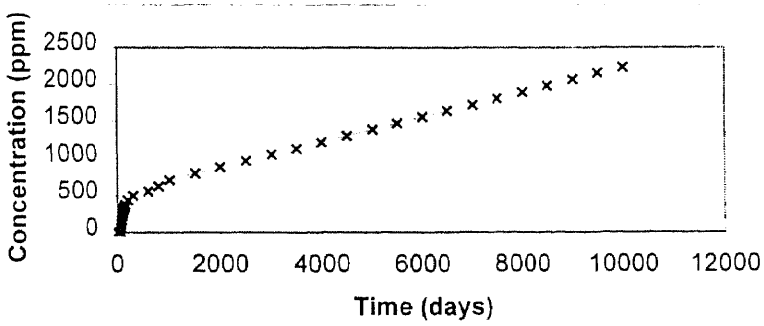

Fig 5.15 Contaminant with Multiple Point Sources Accumulating at the Face of the Wall (Low Permeability Soil) with Poor Construction.

5.3.6 Determination of Risk/Hazard Ratio for Multiple Point Sources

The concentration vs. time data was input to the CalTOX model and cancer risk was determined and presented in Figure 5.16. Maximum permissible value for cancer risk is 10^{-6}. From the results, it is observed that the risk at any time is unacceptable. There is need for remediation. The same conclusion can be reached for the case shown in figure 5.17.

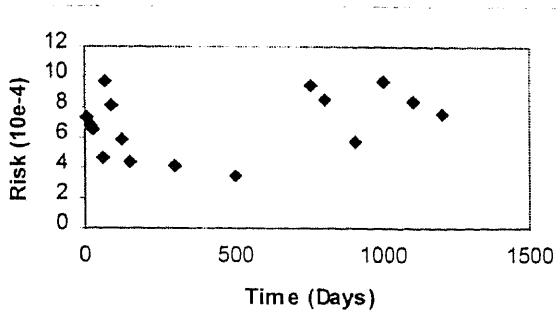

Fig. 5.16 Cancer Risk vs. Time (Contaminant Carried Away from Outer Face of the Wall)

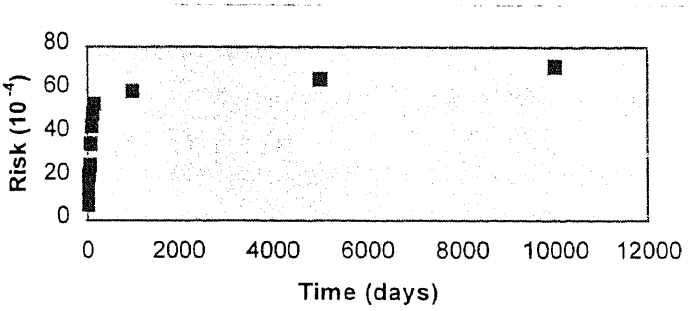

Fig. 5.17 Cancer Risk vs. Time (Contaminant Accumulating at Outer Face of the Wall)

This is a case where treatment is needed. This could be accomplished by treatment of contaminated soil in the site to reduce the risk. It may be possible to determine the concentration of contaminant at the outer and inner face corresponding to acceptable risk. Preliminary determination by CalTOX indicates that the concentration at the outer face is to be 97 ppm.

5.4 Case Study No. 3: Galloway Township Site

5.4.1 Site Description

The geological profile at the Galloway Township site mainly consists of sand. The top layer consists of brown clayey sand 7' thick. This layer is underlain by medium white sand 20' thick. A clayey sand layer 15' thick occurs below the white sand. This clayey sand layer is underlain by medium white sand. Water table was found to be fluctuating between 8' to 20' below the ground level. The surface of the site can be considered to be flat. The hydraulic gradient at the site is less than 0.0005. The targeted contaminant at the site is benzene. The contaminant is located at 20' below the ground level. The thickness of contamination is about 1-2 cm. Contamination at this site is from an underground tank. All the information presented in this section is from literature (USGS, 1995). A peripheral containment system is provided at the site. A schematic diagram of the site is shown in Figure 5.17.

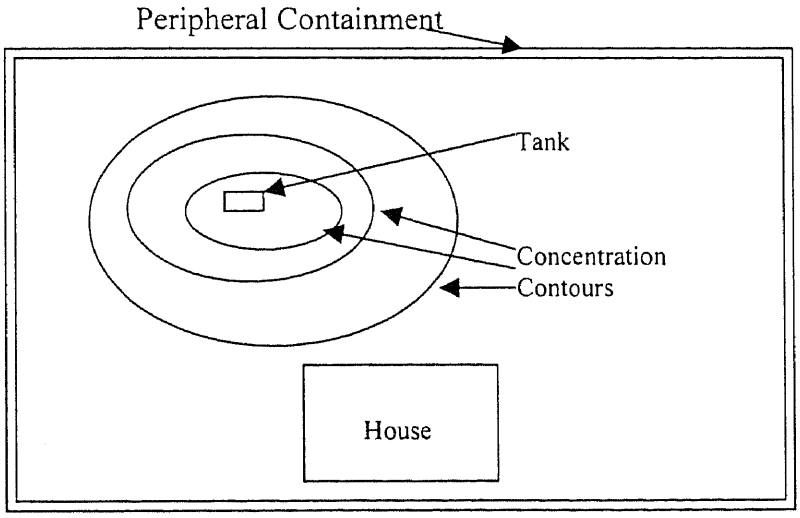

Fig. 5.18 Schematic Diagram of Galloway Township Site

5.4.2 Seepage Velocity

Seepage velocity was calculated from fluctuations in available groundwater data and is shown in Figure 5.19. Steady groundwater table was assumed to be at 20' below ground level. Water level was assumed to fluctuate seasonally above the steady water level. From this data, the hydraulic head was obtained. Gradient was calculated from the hydraulic head and the distance from the source to the peripheral containment. Permeability was estimated for the soil present at the site.

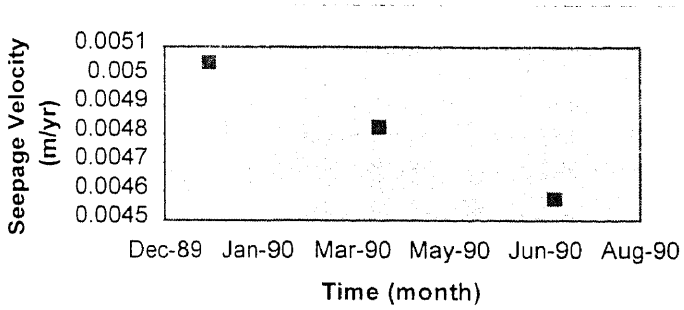

Fig. 5.19 Seepage Velocity vs. Time (Galloway Township)

5.4.3 Source Concentration

Source of contamination is tank at the site. In order to determine the source concentration vs. time plot, quantity of contaminant leaking vs. time graph was generated. Quantity of contaminant leaking at any given time out of the tank was calculated from area of the corresponding concentration contours and corresponding thickness of product. These values were determined for three different dates (January 90, July 90 and April 91) and are shown in figure 5.19. Extrapolating this plot, to zero on the x axis, the time at which the tank started to leak was determined. This is illustrated in the figure 5.20. Utilizing this

information and data from concentration contours, source concentration vs. time plot shown in Fig 5.21 was obtained.

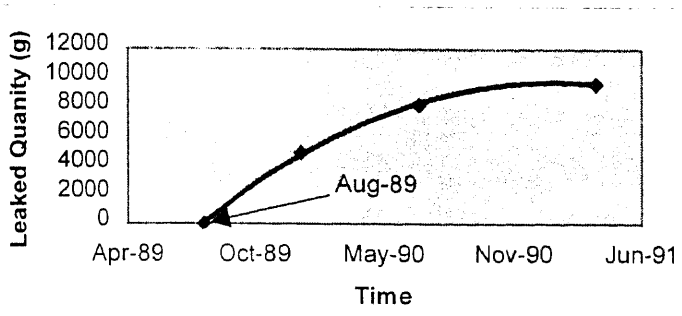

Fig. 5.20 Leaked Contaminant vs. Time

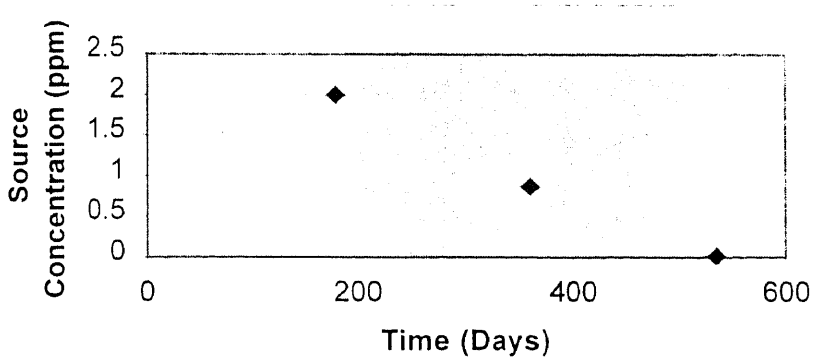

Fig. 5.21 Source Concentration vs. Time

5.4.4 Chemical Gradient

Chemical gradient data utilized here was the same as that used for case history no. 1.

5.4.5 Contaminant Concentration at Inner Surface

Contaminant concentration at inner surface was calculated by equation 5.4. The results follow an exponential trend as shown in figure 5.22.

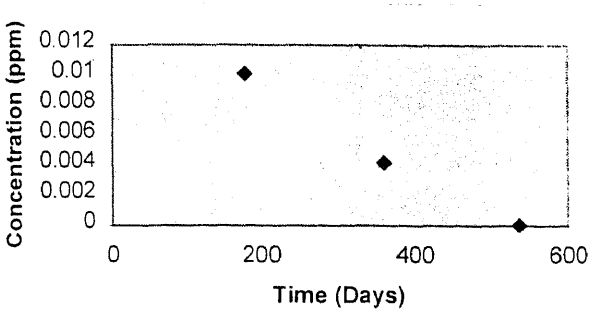

Fig. 5.22 Contaminant Concentration at the Inner Face of the Wall

5.4.6 Contaminant Concentration at Outer Surface

Flow thorough wall was calculated using the equation 3.11, 3.12 and 3.13. The four scenarios utilized for case history no. 1 were considered for this study. Results obtained have been shown in figure 5.23, 5.24, 5.25 and 5.26 respectively.

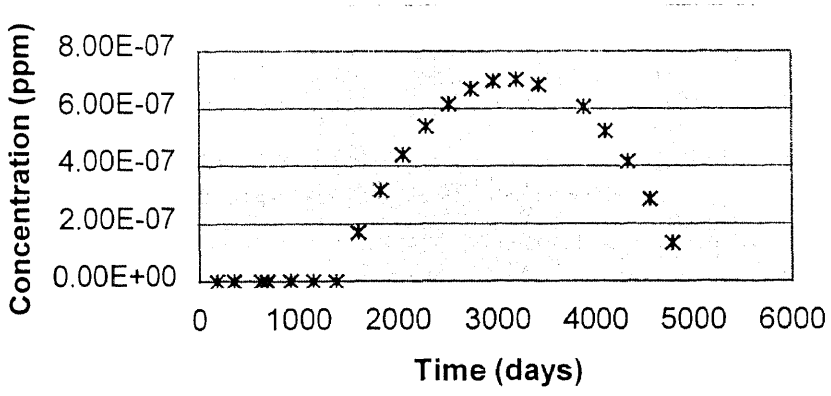

Fig. 5.23 Contaminant Concentration vs. Time, Contaminant Carried Away from the Face of the Wall with Poor Construction

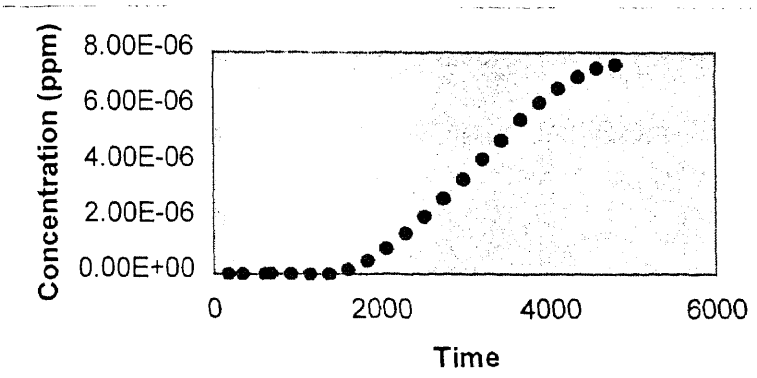

Fig. 5.24 Contaminant Concentration vs. Time, Contaminant Accumulating at the Face of the Wall with Poor Construction

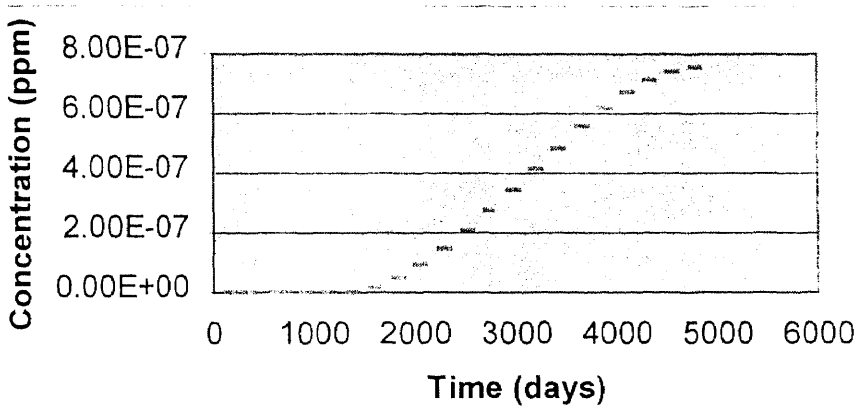

Fig. 5.25 Contaminant Concentration vs. Time, Contaminant Accumulating at the Outer Face of the Wall with Good Construction.

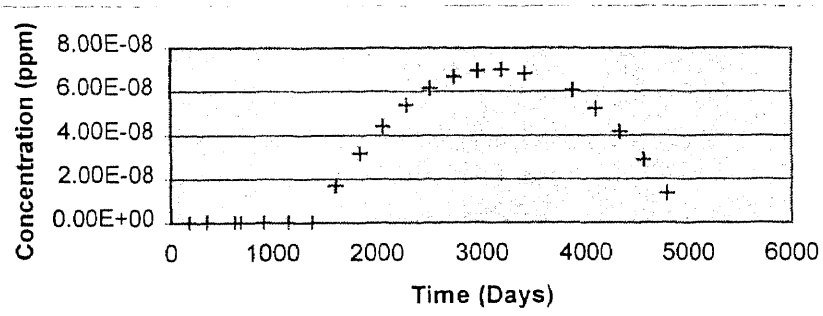

Fig. 5.26 Contaminant Concentration vs. Time, Contaminant Carried Away from the Outer Face of the Wall with Good Construction.

5.4.7 Calculation of Risk/Hazard Ratio

Data from figures 5.23, 5.24, 5.25 and 5.26 were input to CalTOX to calculate cancer risk. Results obtained are presented in figures 5.27, 5.28, 5.29 and 5.30 respectively.

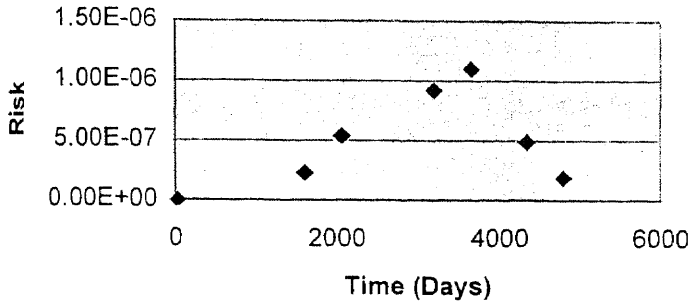

Fig. 5.27 Cancer Risk vs. Time for Contaminant Carried Away from the Face of the Wall with Bad Construction

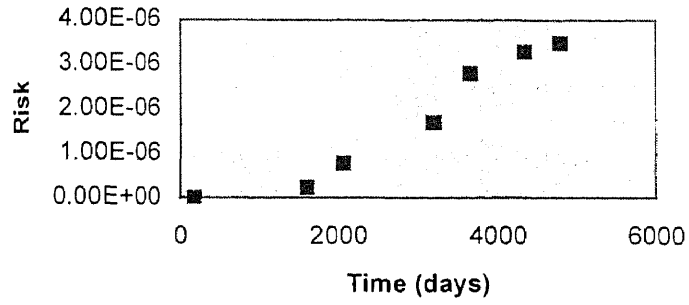

Fig 5.28 Cancer Risk vs. Time for Contaminant Accumulating at the Face of the Wall with Bad Construction

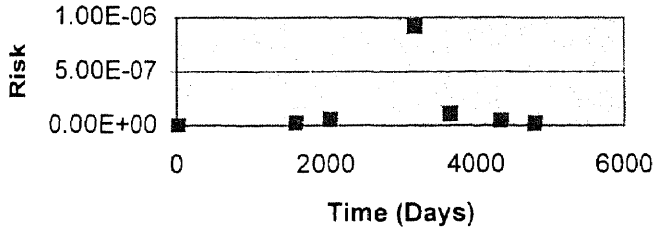

Fig. 5.29 Cancer Risk vs. Time for Contaminant Carried Away from the Face of the Wall with Good Construction

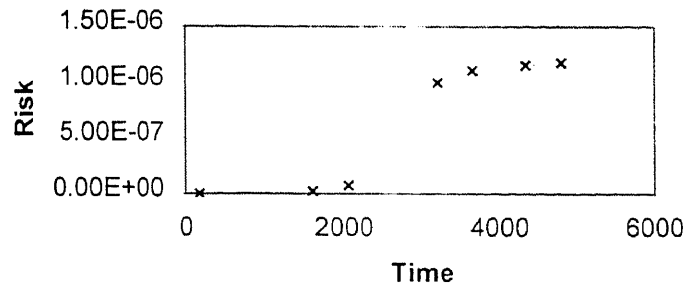

Fig. 5.30 Cancer Risk vs. Time for Contaminant Accumulating at the Face of the Wall with Good Construction

Maximum risk occurs for the condition of wall with bad construction with contaminant accumulating at the outer face of wall. The second worst case also happens for wall with bad construction but with contaminant carried away from the face of the wall. For any of these cases, the risk exceeds allowable limit. Hence QA/QC for construction is necessary and essential. For good construction with contaminant accumulating behind the outer face of wall, the risk is higher than that acceptable for a period of time over 3000 days. For this case, remediation is essential. Hence it becomes obvious that with good construction and collecting the contaminant flowing through the outer face would keep risk lower than that allowable.

CHAPTER 6

RESULTS AND DISCUSSIONS FOR FLOW TOWARDS AND THROUGH SURFACE CONTAINMENTS

6.1. Preamble

In this chapter, implementation of the model proposed in chapter 4 and application of this model to two case studies have been presented. Contaminant concentrations at the lower faces of the top containment have been calculated. This data was provided to the CalTOX model to determine risk. Results obtained have been discussed.

6.2. Case Study Number 1

6.2.1. Introduction

The model developed for this research was applied to a hypothetical site. Three different soil conditions, (sandy soil, silty soil and clayey soil) were assumed at the site. For each case, the time required for maximum capillary rise to occur was determined by solving the Richard's equation with the model developed for this study. Soil suction (matric suction) characteristics for sand, silt and clay were obtained from Literature (Jury et.al., 1990, Nakano et.al., 1986)

6.2.2. Input Data for the Program

Input data was provided as an input file. Initial volumetric water content profile, soil suction and water content-permeability curves, height of maximum capillary rise, maximum time (maximum time is the time after which the program will be terminated), Δz, and Δt have been provided. This has been shown in tables 6.1, 6.2 and 6.3 below:

Table 6.1 Input File for Sand

Item	No
Maximum Value of Coefficient of Permeability(cm/day)	100
Maximum Value of Matric Suction (cm)	345
Maximum Value of Capillary Rise(cm)	15
Δz (cm)	2.5
Δt (days)	0.0000452
Maximum time (days)	15
Number of Nodes	6

Initial Water Content Profile	Coefficient of Permeability (cm/day)	Soil Suction (cm)
0.1	0.003	345.0
0.15	0.11	148.0
0.25	2.6	47.0
0.3	8.2	27.0
0.35	25.0	13.0
0.4	100.0	0.0

Table 6.2 Input Data for Silt

Item	No
Maximum Value of Coefficient of Permeability (cm/day)	1
Maximum Value of Matric Suction (cm)	10000
Maximum Value of Capillary Rise (cm)	102
Δz (cm)	25.5
Δt (days)	1.5
Maximum time (days)	735
Number of Nodes	4

Initial Water Content Profile	Coefficient of Permeability (cm/day)	Soil Suction (cm)
0.1	0.001	10000.0
0.2	0.005	900.0
0.3	0.01	500.0
0.4	0.8	80.0

Table 6.3 Input Data for Clay

Item	No
Maximum Value of Coefficient of Permeability (cm/day)	0.1
Maximum Value of Matric Suction (cm)	100000
Maximum Value of Capillary Rise (cm)	300
Δz (cm)	50
Δt (days)	3
Maximum time (days)	3650
Number of Nodes	6

Initial Water Content Profile	Coefficient of Permeability (cm/day)	Soil Suction (cm)
0.25	0.001	100000.0
0.30	0.01	20000.0
0.35	0.08	10000.0
0.4	0.085	8000.0
0.45	0.09	5000.0
0.5	0.1	1000.0

Maximum capillary rise is calculated based upon following equation: (Bear and Verrujit 1990)

$$H_c = [0.45/D_{10}]\{(1-n)/n\} \qquad (6.1)$$

Where,

H_c is maximum capillary rise.

D_{10} = Diameter corresponding to 10% finer.

n is Porosity .

For this case history, D_{10} values of 0.045 mm, 0.00225 mm and 0.0012 mm were assumed for typical sand, silt and clay respectively. Porosity values of 0.4, 0.4 and 0.55 were assumed for sand, silt and clay respectively.

6.2.3 Results Obtained and Discussion of Results

It is seen from the results that at the end of the maximum time specified for the program, the volumetric water contents at the topmost layer became almost equal to those at 100% saturation. For the purpose of this study, the time for maximum capillary rise to occur was determined as time at which the value of volumetric water content for the top layer did not change in sixth decimal for fifteen successive time steps.

The times for maximum capillary rise to occur determined from the results and those computed form Terzaghi's equation are shown in table 6.4.

$$t = n * h / k (Ln(h/h-z) - z/h) \qquad (6.2)$$

Where,

t = time required for meniscus of capillary water to rise to the height z above the free water level,

n = porosity,

k = coefficient of permeability,

h = height of capillary rise,

z = distance of capillary meniscus from groundwater level.

The value of k was taken as 10^{-2} cm/s for sand, 10^{-5} cm/s for silt, 7.5 * 10^{-6} cm/s for clay. The values of capillary rise were calculated by equation 6.1 and are 15 cm, 102 cm and 300 cm for sand silt and clay respectively.

Table 6.4 The time for maximum capillary rise obtained from the results and corresponding values computed from Terzaghi's Equation, Predictor Corrector Method, Forward Difference Method.

Material	Unit	Time Required for Maximum Capillary Rise		
		Terzaghi's Equation	Predictor Corrector	Forward Difference
Sand	(Hours)	10.5	1.03	0.25
Silt	(Days)	605	99	27
Clay	(Days)	17777	2187	581

In order to validate the results by an independent source, the time taken for capillary rise to occur computed from Terzaghi's equation was compared with that from Richard's equation. The differences in between these values can be explained as follows: Terzaghi's equation (Equation 6.2) has some limitations. First of all, it does not consider the degree of saturation. The permeability value is assumed as constant even though it changes with degree of saturation. Terzaghi's equation assumes maximum suction in the capillary zone as H_c the height of capillary rise. This means that Terzaghi's equation considers matric suction as a product of density of water and capillary rise, which is not true. All of these above limitations are overcome by Richard's equation.

6.2.3.1 Effect of Diffusivity on Results: The problem was solved for diffusivity values of 0.0625, 0.125, 0.25 and 0.5 respectively. Final volumetric water contents for the top layer for these different values are presented in the tables 6.5 through 6.7 respectively. It is seen that these results were not practically affected by diffusivity values in the range considered.

Table 6.5 Effect of Diffusivity Volumetric Water Content on Sand at t. = 1.03 Hours.

Volumetric Water Content					Value at 100% Saturation
	Diffusivity 0.0625	Diffusivity 0.125	Diffusivity 0.25	Diffusivity 0.5	
Time t = 0					
0.1	0.399984	0.399993	0.399997	0.399998	0.4

Table 6.6 Effect of Diffusivity Volumetric Water Content on Silt at t = 99 Days

Volumetric Water Content					Value at 100% Saturation
	Diffusivity 0.0625	Diffusivity 0.125	Diffusivity 0.25	Diffusivity 0.5	
Time t = 0					
	(Days)	(Days)	(Days)	(Days)	
0.1	0.399997	0.399999	0.399999	0.399999	0.4

Table 6.7 Effect of Diffusivity Volumetric Water Content on Clay at t = 2187 Days

Volumetric Water Content					Value at 100% Saturation
Time t = 0	Diffusivity 0.0625	Diffusivity 0.125	Diffusivity 0.25	Diffusivity 0.5	
0.25	0.499898	0.499901	0.499945	0.499997	0.5

For some initial value problems, diffusion coefficient values of 0.25 have been recommended (Adina Software Manual, 1995). Based on the results of this study, a decision has been made to use the results obtained with a diffusivity coefficient of 0.125.

6.2.3.2 Effect of Δz/h on Results: The formulation proposed in this study for the solution of Richard's equation is a function of diffusivity and Δz/h. In the previous section, the effect of diffusivity on the results was presented. Now the effect of Δz/h on the results will be discussed.

The problem was solved for sand, silt and clay for diffusivity of 0.125 in the following manner.

a. For sand, with Δz/h = 0.17, 0.25 and 0.5.

b. For silt, with Δz/h = 0.0833, 0.17, 0.25 and 0.33.

c. For clay, with Δz/h = 0.0833, 0.17, 0.25 and 0.33

Values of water content at the top layer for these conditions are presented in tables 6.8, 6.9 and 6.10 respectively.

Table 6.8 Volumetric Water Content at the top of Capillary Surface for Sands after 1.03 Hours

Volumetric Water Content				Value at 100% Saturation
Time t = 0	Δz/H 0.125	Δz/H 0.25	Δz/H 0.5	
0.1	0.399993	0.399997	0.399998	0.4

Table 6.9 Volumetric Water Content at the top of Capillary Surface for Silts after 99 days

Volumetric Water Content					Value at 100% Saturation
Time t = 0	Δz/H 0.0833	Δz/H 0.17	Δz/H 0.25	Δz/H 0.33	
0.1	0.399997	0.399997	0.399997	0.4	0.4

Table 6.10 Volumetric Water Content at the top of Capillary Surface for Clays after 2187 days

Volumetric Water Content					Value at 100% Saturation
Time t = 0	Δz/H 0.0833	Δz/H 0.17	Δz/H 0.25	Δz/H 0.33	
0.25	0.499961	0.499945	0.499898	0.499801	0.5

Based on these results, a Δz/h value of 0.17 was chosen for this study. Thus the permeability grid constant value of (1/8) (1/6) = (1/48) is utilized. For this condition, the final volumetric water contents at the top layer for different time intervals have been shown in tables 6.11 through 6.13 respectively. These results are plotted in Figures 6.1 through 6.3 respectively. This plot illustrates that the capillary rise in silt and clay take a very long time to occur. During this time, water table can fluctuate and can cause conditions to change. In these materials, thus capillary action never fully materializes. For risk determination, it is thus sufficient to assume the water table to be constant and at the highest level based on seasonal fluctuations. From the water content profiles, the quantity of contaminant moving in upward direction can be calculated. The results can be provided to CalTOX model to calculate the risk or hazard ratio.

Table 6.11 Water Content Profile for sand at diffusivity = 0.125 and $\Delta z/h = 0.17$

Depth	T = 0	t = 0.0011 Hours	t=0.52 Hours	t=1.03 Hours
2.5	0.1	0.100001	0.277458	0.399993
5	0.15	0.150025	0.397734	0.399996
7.5	0.25	0.250056	0.399892	0.399997
10	0.3	0.300169	0.399988	0.399998
12.5	0.35	0.350753	0.399999	0.399999
15	0.4	0.4	0.4	0.4

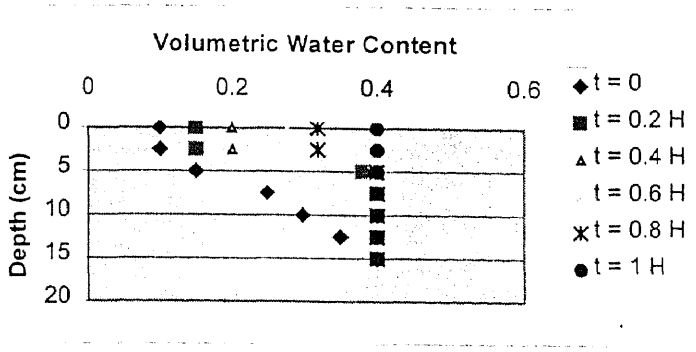

Fig. 6.1 Depth vs. Water Content for Sand

Table 6.12 Water Content Profile for silt at diffusivity = 0.125 and $\Delta z/h = 0.17$

Depth	T = 0	t = 1.6 days	t=45 days	t=99 days
25.5	0.1	0.100072	0.113023	0.399999
51	0.2	0.200253	0.319173	0.4
76.5	0.3	0.300916	0.399959	0.4
102	0.4	0.4	0.4	0.4

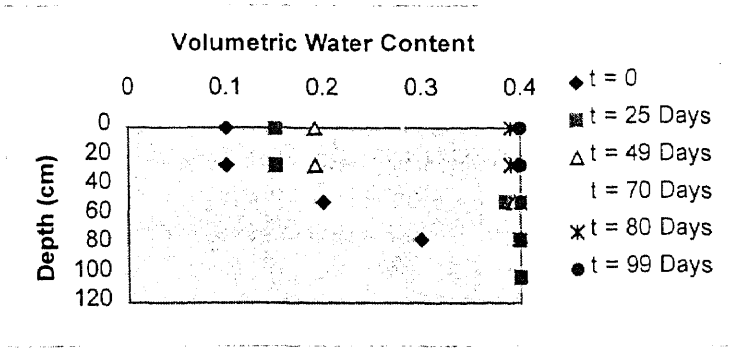

Fig. 6.2 Depth vs. Water Content for Silt

Table 6.13 Water Content Profile for clay at diffusivity = 0.125 and $\Delta z/h = 0.17$

Depth	T = 0	t = 3 days	t=1093 days	T=2187 days
50	0.25	0.25045	0.475001	0.499901
100	0.3	0.3035	0.492274	0.499978
150	0.35	0.35025	0.498047	0.499995
200	0.4	0.40025	0.49964	0.499997
250	0.45	0.4505	0.499964	0.499999
300	0.5	0.5	0.5	0.5

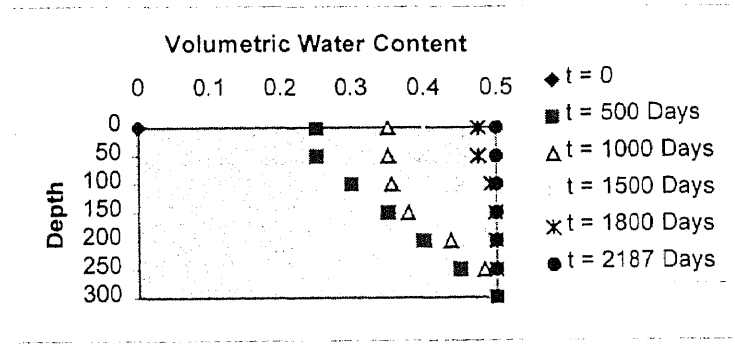

Fig. 6.3 Depth vs. Water Content for Clay

6.3 Case Study No. 2

6.3.1 Site Description

The site is located in Northern New Jersey. The top 5'-10' below the ground level is fill consisting of slag, cinder, fine sand with traces of gravel. This is underlain by an 8' thick clayey silt layer with traces of sand. Below this, brown peat was encountered. Water table fluctuates between 5'to 10' below the ground level. For this study, the highest location of water table (5' below ground level) is assumed. This has been done to include the effect of infiltration due to rain on water table. Soil was modeled as fine silty sand in the zone of capillary rise and suction and permeability characteristics utilized for this study were obtained from literature. (Jury, Gardner and Gardener, 1990, Houston, 1995, 1997). Maximum height of capillary rise was computed from equation 6.1 with D_{10} equal to 0.0045 and n equal to 0.4. The target contaminants at the site were Cr^{3+} and Cr^{6+}. Chromium was detected at approximately 5' below the soil. The concentration of contaminant (hexavalent chromium) was observed to be varying from 4 ppm to 40 ppm in groundwater. For the purpose of risk calculations, a maximum concentration of 40 ppm of Cr^{6+} has been assumed. A subsurface profile for the site is shown in Fig. 6.4.

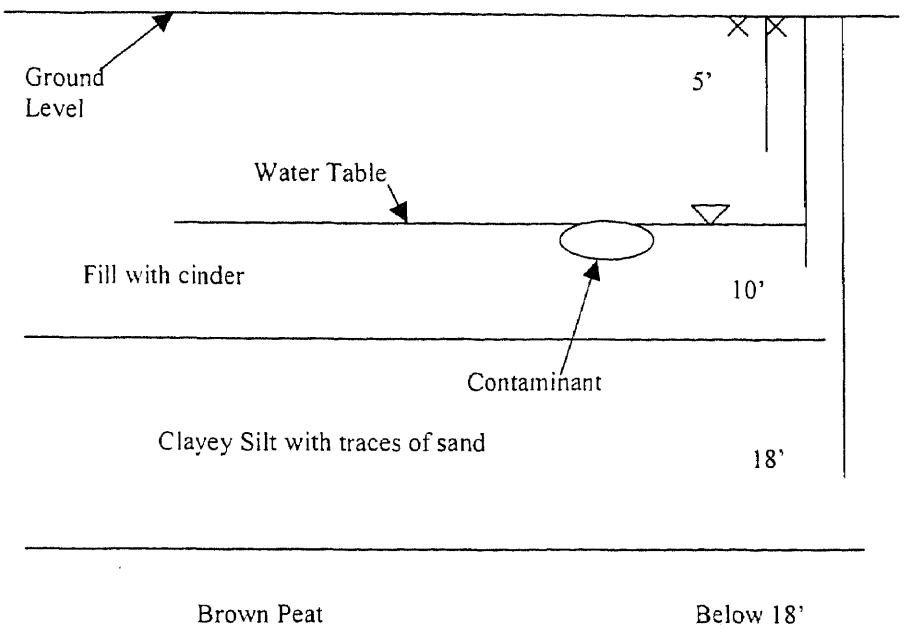

Fig. 6.4 Subsurface Profile for Case Study No. 2

6.3.2 Input File

The input file is provided as below:

Table 6.14 Input file for Case History Number 2

Item	No
Maximum Value of Coefficient Permeability (cm/day)	100
Maximum Value of Matric Suction (cm)	345
Maximum Value of Capillary Rise (cm)	150
Δz (cm)	25
Δt (days)	0.0000452
Maximum Time (days)	0.5
No. of Nodes	6

Initial Water Content Profile	Coefficient of Permeability (cm/day)	Soil Suction (cm)
0.1	0.003	345.0
0.15	0.11	148.0
0.25	2.6	47.0
0.3	8.2	27.0
0.35	25.0	13.0
0.4	100.0	0.0

6.3.3 Results Obtained and Discussion of Results

The problem was solved for diffusivity values of 0.0625, 0.125, 0.25 and 0.5 respectively with predictor corrector and forward difference techniques. Final volumetric water content values for the top layer for these different values obtained from predictor corrector method are presented in the Table 6.15. It is seen that these results were not practically affected by diffusivity values in the range considered. Hence it was decided to use a diffusivity value of 0.125.

Table 6.15 Effect of Diffusivity on Volumetric Water Content after 1.03 hours

Volumetric Water Content					Value at 100% Saturation
Time t = 0	Diffusivity 0.0625	Diffusivity 0.125	Diffusivity 0.25	Diffusivity 0.5	
0.1	0.399984	0.399993	0.399997	0.399998	0.4

For a diffusivity value of 0.125, water content profiles were obtained for different values of $\Delta z/H$. Results obtained are presented in Table 6.16.

Table 6.16 Volumetric Water Content at the top of Capillary Surface for Case Study No. 2 after 1.03 Hours

Volumetric Water Content				Value at 100% Saturation
Time t = 0	Δz/H 0.17	Δz/H 0.22	Δz/H 0.33	
0.1	0.399993	0.399997	0.399998	0.4

Based on these results, it was decided to use the results obtained with a diffusivity value of 0.125 and Δz/h = 0.17. Water content vs. depth values for these conditions are shown in Table 6.17. For these conditions, the water content profile obtained is shown in figure 6.5.

Results obtained indicate that the maximum capillary rise occurs in about 1.03 hours. At this time, since height of capillary rise is 5', soil at the ground surface becomes completely saturated by capillary action. Hexavalent chromium dissolved in water moves upto the ground surface due to capillary effects. Then water level drops, causing the top level of capillary zone to fall below ground level. Change in water pressure decreases the solubility of hexavalent chromium, which then comes out of solution. This causes streaks of chromium, yellow and green in color, to appear at the ground surface. This phenomenon has been discussed in the literature (Raghu and Hsieh, 1989).

Observations at site indicate that streaks of chromium appear after 2 to 3 hours after rain. Our results show the time for maximum capillary rise to be 1.03 hours. This rise occurs after water table rises by infiltration. Accounting for times for infiltration and capillary rise obtained from our study, a period of 2-3 hours for the occurrence of streaks after rain seems reasonable.

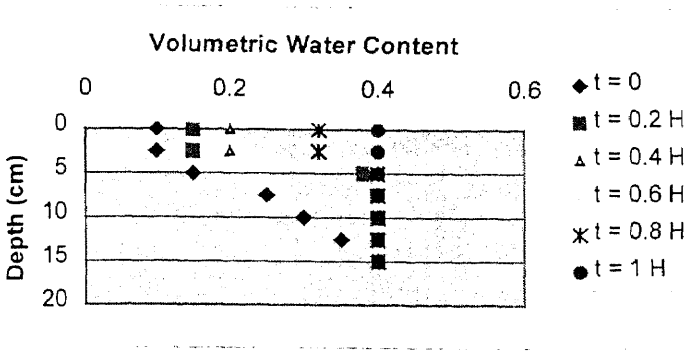

Fig. 6.5 Depth vs. Water Content for Case Study No. 2

From the results of water contents presented in Table 6.17 and in Figure 6.6, the contaminant concentrations as a function of time can be determined and are presented in Figure 6.7. These results are input to CalTOX model.

Table 6.17 Volumetric Water Content Profile for diffusivity = 0.125 and $\Delta z/h = 0.17$

Depth	T = 0	t = 0.0011 Hours	t=0.52 Hours	t=1.03 Hours
25	0.1	0.100001	0.277458	0.399993
50	0.15	0.150025	0.397734	0.399996
75	0.25	0.250056	0.399892	0.399997
100	0.3	0.300169	0.399988	0.399998
125	0.35	0.350753	0.399999	0.399999
150	0.4	0.4	0.4	0.4

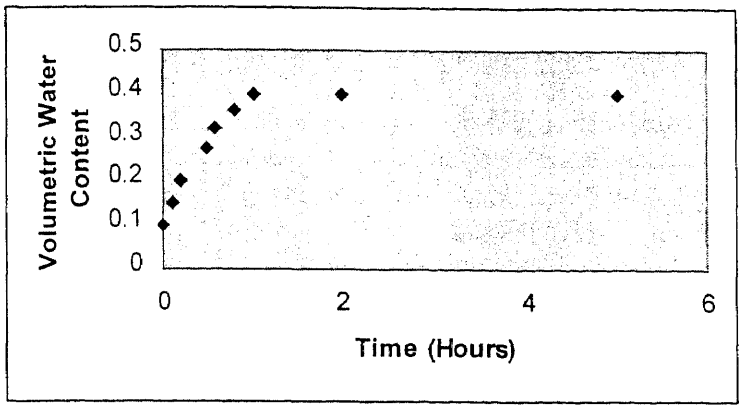

Fig. 6.6 Volumetric Water Content vs. Time

6.3.4 Calculation of Risk

For determination of risk due to hexavalent chromium contamination, the model developed in section 4.8.1 of this study was used. Results are presented in figure 6.8. It is seen that maximum risk occurs about 1 hour after rain and it is acceptable.

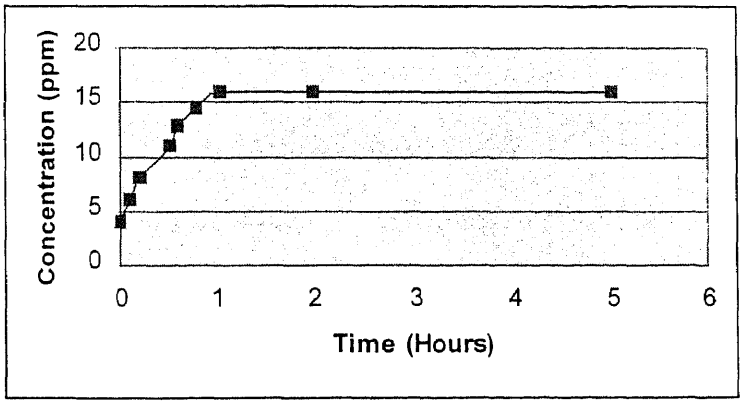

Fig. 6.7 Concentration vs. Time for Case Study No. 2

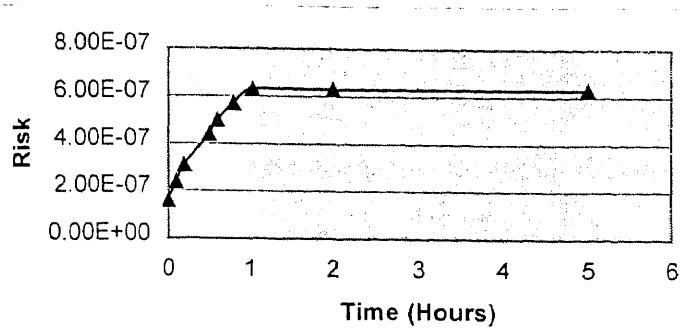

Fig 6.8 Risk vs. Time for Case Study Number 2

The preceding sections discussed the contaminant concentration at the inner face of cap. When the cap cracks, the contaminants reach the outer face of cap. In order to determine this, occurrence of degradation of cap is discussed in the following section.

6.4 Strategies for Development based on Model

Results obtained from this model yield the risk as a function of time. Most often, risk is acceptable in the beginning. As the contaminant travels to the top, the risk becomes unacceptable. This could be mitigated in the following three ways:

1. By treating the contaminant and reducing the contaminant concentration so that the risk is acceptable, since risk can be calculated by our model as a function of contaminant concentration,

2. By providing a capillary break at the bottom of the cap and collecting the contaminant. Periodically, the concentrations of contaminants can be monitored. When the contaminant concentration increases, it can be pumped out for treatment and proper disposal. Our model can provide guidance and information required for this option and

3. By increasing the height of fill and preventing capillary rise to the top. Our model can determine contaminant concentration and risk for this option also.

Before developing the Brownfield site, the above options can be considered. The most feasible option would be the one that is practical, economical and for which the risk is acceptable. The most appropriate strategy can be chosen for development.

CHAPTER 7

CONCLUSION

7.1 Conclusions

Based on this study, following conclusions can be drawn,

1. It is possible to develop a process based model for transport of contaminants towards and through peripheral containments that can include the processes such as advection and diffusion. Quality of construction and aging of walls can be also incorporated in the model. The concentrations of contaminant can be calculated at the inner and outer face of the containment. Equations were developed for flow of contaminants through containments. These concentrations can be provided as input to CalTOX model for determination of risk as a function of time. CalTOX model utilizes residential exposure scenario for organic chemicals. However, the same model can be modified for industrial exposure scenario and inorganic compounds or metals.
2. It is possible to apply Richard's equation that is nonlinear transient partial differential equation of the parabolic type, to capillary phenomena in soils. The solution of this equation can be obtained by finite difference technique. Various properties of soil such as permeability, soil suction can be obtained from the laboratory tests as well as literature and can be provided to the model. Water content profiles in vadoze zone can be obtained as function of time. Based upon this, the concentrations of contaminant can be determined. These data can be provided to CalTOX model and risk due to surface containment can be calculated.

3. The recommended values for diffusivity and permeability grid constant for solving Richard's equation are respectively 1/8 and 1/48.

7.2 Recommendation for Future Study

Following topics may be considered for future research,

1. Laboratory studies to determine capillary rise as a function of time.
2. More field verification of the results of model.
3. Laboratory and literature studies for evaluation of diffusion coefficient and verification of correlation between diffusion coefficient, coefficient of consolidation and molecular weight.

APPENDIX A

DERIVATIONS

A.1 Contaminant Flow through the Wall

This is assumed to occur both by advection and dispersion.

$C_o(t) = C_i(t)*V_s(t)*n(t) + G(t)*n(t)*D^*$ (A.1)

Since the wall thickness is small,

$G(t) = (C_i(t) - C_o(t)) / h(t)$ (A.2)

Substituting (A.2) in (A.1),

$C_o(t) = C_i(t)* V_s(t)*n(t)+(n(t)*(D^*)*(C_i(t)- C_o(t))/ h(t))$ (A.3)

Simplifying and rearranging terms,

$C_o(t) = (C_i(t)* h(t))(V_s(t)*n(t)+n(t)*(D^*))/(h(t)+n(t)*(D^*))$ (A.4)

Porosity n(t)

T(t) = Thickness fraction at any time t

h(0) = Thickness of wall at time t = 0.

$T(t) = h(t)/h(0)$ (A.5)

$T(t) = h(t)/h(0)$ (A.6)

$= V(t)/V(0)$, since area is assumed to be constant (A.7)

Where,

V(t) = The volume of the wall at any time t.

V(0) = Initial volume of the wall.

Volumetric Strain at any time t,

$\varepsilon_v(t) = (V(0)-V(t))/ V(0)$ (A.8)

$= 1- (Vt)/ V(0))$ (A.9)

$= 1- T(t)$ (A.10)

$= (\delta e/1+e_0)$ (A.11)

Since $\delta e = e(t)-e_0$ (A.12)

From (A.10) and (A.11) above,

$\delta e = (1+e_0)(1- T(t))$ (A.13)

$e(t) = e_0-\delta e = (T(t)(1+e_0))-1$ (A.14)

$n(t) = e(t)/(1+ e(t))$ (A.15)

$= ((T(t)(1+e_0))-1)/(T(t)(1+e_0))$ (A.16)

A.2 Relationship between Volumetric Water Content and Gravimetric Water Content

$$\theta v = Vw/V = S\,n \quad (A.17)$$

$$S = w\,Gs/\,e \quad (A.18)$$

$$e = Vv/Vs \quad (A.19)$$

$$\theta v = w\,Gs\;\; Vv/V\;\; Vs/Vv \quad (A.20)$$

$$= w\,Gs\;Vs/V \quad (A.21)$$

$$= w\,Gs\,(V - Vv)/V \quad (A.22)$$

$$= w\,Gs\,(1 - n) \quad (A.23)$$

$$= (w\,Gs\,/\,S)\,S\,(1-n) \quad (A.24)$$

APPENDIX B

FINITE DIFFERENCE FORMULATION FOR SOLUTION OF RICHARD'S EQUATION

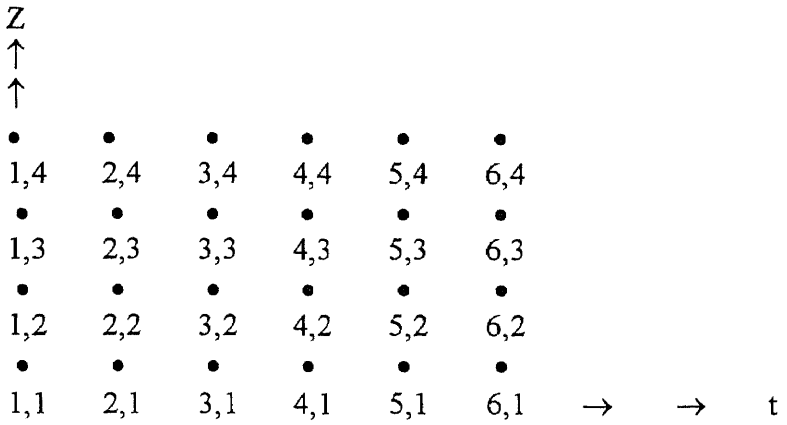

Fig B.1: Nodes for Finite Difference Formulation

Legend: • Node and → → t direction, ↑↑ Z Direction

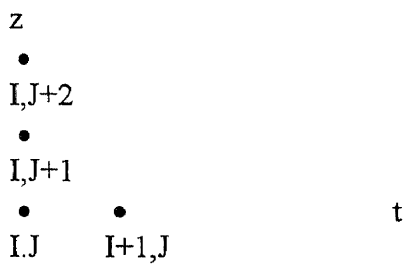

Fig B.2: Nodes for finite difference formulation at node I, J

Derivatives are computed by forward difference.

$$(\partial\theta/\partial t)\ @\ I,J = (\theta(I+1,J) - \theta(I,J))/\Delta t \quad \text{(B.1)}$$

$$\theta(I+1,J) = \theta(I,J) + ((\partial\theta/\partial t)\ @\ I,J)\ \Delta t \quad \text{(B.2)}$$

$$(\partial\theta/\partial t) = \partial/\partial z\ (k(\partial h/\partial z) + 1) \quad \text{(B.3)}$$

$$(\partial\theta/\partial t) = \partial p/\partial z, \text{ where } p = (k(\partial h/\partial z) + 1) \quad \text{(B.4)}$$

$$(\partial\theta/\partial t)\ @\ I.J = \partial p/\partial z\ @\ I, J \quad \text{(B.5)}$$

$$= (p(I,J+1) - p(I,J))/\Delta z \quad \text{(B.6)}$$

$$p(I,J) = k(I,J)(((\partial h/\partial z)@I,J) + 1) \quad \text{(B.7)}$$

$$p(I,J+1) = k(I,J+1)(((\partial h/\partial z)@I,J+1) + 1) \quad \text{(B.8)}$$

$$(\partial h/\partial z)@I,J = (h(I,J+1) - h(I,J))/\Delta z \quad \text{(B.9)}$$

$$(\partial h/\partial z)@I,J+1 = (h(I,J+2) - h(I,J+1))/\Delta z \quad \text{(B.10)}$$

$$p(I,J) = k(I,J)\,(((h(I,J+1)-h(I,J))/\Delta z) + 1) \quad \text{(B.11)}$$

$$p(I,J) = k(I,J)\,((h(I,J+1)-h(I,J)+\Delta z)/\Delta z) \quad \text{(B.12)}$$

$$p(I,J) = (k(I,J)/\Delta z)\;(h(I,J+1)-h(I,J)+\Delta z) \quad \text{(B.13)}$$

$$p(I,J+1) = (k(I,J+1)/\Delta z)\;(h(I,J+2)-h(I,J+1)+\Delta z) \quad \text{(B.14)}$$

$$(p(I,J+1)-p(I,J))/\Delta z = (1/\Delta z)(1/\Delta z)(k(I,J+1)\,h(I,J+2)- k(I,J+1)\,h(I,J+1)+ k(I,J+1)\,\Delta z- k(I,J)\,h(I,J+1)+ k(I,J)\,h(I,J) - k(I,J)\,\Delta z) \quad \text{(B.15)}$$

Normalize $\mathbf{k}(I,J) = k(I,J)/K$ where K is saturated Permeability (B.16)

$\mathbf{h}(I,J) = h(I,J)/H$ where H is the maximum Capillary rise (B.17)

$\Delta\mathbf{z} = \Delta z/H$ (B.18)

$\mathbf{k}(I,J)$, $\mathbf{h}(I,J)$, $\Delta\mathbf{z}$ are defined as respectively normalized permeability, normalized suction and normalized node thickness.

$$(p(I,J+1)-p(I,J))/\Delta z = (KH/\Delta z^2)(\mathbf{k}(I,J+1)\,\mathbf{h}(I,J+2)- \mathbf{k}(I,J+1)\,\mathbf{h}(I,J+1) + \mathbf{k}(I,J+1)\,\Delta\mathbf{z}-\mathbf{k}(I,J)\,\mathbf{h}(I,J+1)+ \mathbf{k}(I,J)\,\mathbf{h}(I,J) - \mathbf{k}(I,J)\,\Delta\mathbf{z}) \quad \text{(B.19)}$$

$$(\partial\theta/\partial t)\ @\ I.J = (KH/\Delta z^2)(\mathbf{k}(I,J+1)\,\mathbf{h}(I,J+2)- \mathbf{k}(I,J+1)\,\mathbf{h}(I,J+1) + \mathbf{k}(I,J+1)\,\Delta\mathbf{z}-\mathbf{k}(I,J)\,\mathbf{h}(I,J+1)+ \mathbf{k}(I,J)\,\mathbf{h}(I,J) - \mathbf{k}(I,J)\,\Delta\mathbf{z}) \quad \text{(B.20)}$$

$$\theta(I+1,J) =\theta(I,J)+(KH\Delta t/\Delta z^2)\,(\mathbf{k}(I,J+1)\,\mathbf{h}(I,J+2)- \mathbf{k}(I,J+1)\,\mathbf{h}(I,J+1) + \mathbf{k}(I,J+1)\,\Delta\mathbf{z}-\mathbf{k}(I,J)\,\mathbf{h}(I,J+1)+ \mathbf{k}(I,J)\,\mathbf{h}(I,J) - \mathbf{k}(I,J)\,\Delta\mathbf{z}) \quad \text{(B.21)}$$

$$\theta(I+1,J) =\theta(I,J)+(KH\Delta t/\Delta z^2)\,(\mathbf{k}(I,J+1)\,\mathbf{h}(I,J+2)- \mathbf{k}(I,J+1)\,\mathbf{h}(I,J+1) -\mathbf{k}(I,J)\,\mathbf{h}(I,J+1)+ \mathbf{k}(I,J)\,\mathbf{h}(I,J) +\Delta\mathbf{z}\,(\mathbf{k}(I,J+1)- \mathbf{k}(I,J))) \quad \text{(B.22)}$$

All bold quantities are dimensionless as well as $(KH\Delta t/\Delta z^2)$

$(KH\Delta t/\Delta z^2)$ is similar to time factor T_v in consolidation where $T_v = C_v\,t/z^2$

$$\theta(I+1,J) -\theta(I,J)=(KH\Delta t/\Delta z^2)\,(\mathbf{k}(I,J+1)\,\mathbf{h}(I,J+2)- \mathbf{k}(I,J+1)\,\mathbf{h}(I,J+1) -\mathbf{k}(I,J)\,\mathbf{h}(I,J+1)+ \mathbf{k}(I,J)\,\mathbf{h}(I,J) +\Delta\mathbf{z}\,(\mathbf{k}(I,J+1)- \mathbf{k}(I,J))) \quad \text{(B.23)}$$

$$\theta(I+1,J) -\theta(I,J)=Tc\,(\mathbf{k}(I,J+1)\,\mathbf{h}(I,J+2)- \mathbf{k}(I,J+1)\,\mathbf{h}(I,J+1) -\mathbf{k}(I,J)\,\mathbf{h}(I,J+1) +\mathbf{k}(I,J)\,\mathbf{h}(I,J) +\Delta\mathbf{z}\,(\mathbf{k}(I,J+1)- \mathbf{k}(I,J))) \quad \text{(B.24)}$$

It will be interesting to see as to how $(\theta(I+1,J) -\theta(I,J)$ vs T_c plots come out.

$$(\theta(I+1,J) -\theta(I,J))/\Delta t=(KH/\Delta z^2)(\mathbf{k}(I,J+1)\,\mathbf{h}(I,J+2)- \mathbf{k}(I,J+1)\,\mathbf{h}(I,J+1) -\mathbf{k}(I,J)\mathbf{h}(I,J+1) +\mathbf{k}(I,J)\,\mathbf{h}(I,J) +\Delta\mathbf{z}\,(\mathbf{k}(I,J+1)- \mathbf{k}(I,J))) \quad \text{(B.25)}$$

$(\partial\theta/\partial t) = \partial^2 Dw(\theta)/\partial z^2 + \partial k(\theta)/\partial z$ can be seen from (B25)

$$((k(I,J+1)\,h(I,J+2)- k(I,J+1)\,h(I,J+1) -k(I,J)h(I,J+1) +k(I,J)\,h(I,J))/\Delta z^2=\partial^2 Dw(\theta)/\partial z^2 \quad \text{(B.26)}$$

$$(k(I,J+1)- k(I,J)/\Delta z\,) =\partial k(\theta)/\partial z \quad \text{(B.27)}$$

Equation (B.24) can be rewritten as:

$$\Delta\theta = T_c\,(\mathbf{k}(I,J+1)\,\mathbf{h}(I,J+2)- \mathbf{k}(I,J+1)\,\mathbf{h}(I,J+1) -\mathbf{k}(I,J)\mathbf{h}(I,J+1) +\mathbf{k}(I,J)\,\mathbf{h}(I,J)) +$$

$$(T_c\Delta z\ (\mathbf{k}(I,J+1)-\ \mathbf{k}(I,J)) \quad \text{(B.28)}$$

$$\Delta\theta \quad = T_c\ (c_1+c_2) \quad \text{(B.29)}$$

$$c_1 \quad = (\mathbf{k}(I,J+1)\ \mathbf{h}(I,J+2)-\ \mathbf{k}(I,J+1)\ \mathbf{h}(I,J+1)\ -\mathbf{k}(I,J)\mathbf{h}(I,J+1)\ +\mathbf{k}(I,J)\ \mathbf{h}(I,J)) \quad \text{(B.30)}$$

$$c_2 \quad = \Delta\mathbf{z}\ (\mathbf{k}(I,J+1)-\ \mathbf{k}(I,J)) \quad \text{(B.31)}$$

$$T_c\Delta\mathbf{z} = (KH\Delta t/\Delta z^2)\ (\Delta z/H) = (K\Delta t/\Delta z) = T_k, \text{a dimensionless factor} \quad \text{(B.32)}$$

APPENDIX C

ACTIVITY EQUATIONS

$A = f/P^S$ (C.1)

A = Activity
f = fugacity
P^S = Vapor Pressure

Overall Mass Balance equations

Unsteady State

Sediment Balance

$VS\ ABS\ dAS/dt = AW(DD + DT) - AS(DR + DT + DS + DS)$ (C.2)

Water Balance

$VW\ ABW\ dAW/dt = AA(DV + DQ + DC + DM) + AS(DR + DT) + FI(DI + DX) + EW - AW(DV + DW + DD + DJ + DY + DT)$ (C.3)

Steady State Equations

Water Balance

$$AW = (EW + AA + (DV + DQ + DC + DM) + AI(DI + DX))/ ((DV + DW + DD + DJ + DY + DT) - ((DR + DT)(DD + DT)/(D[illegible] + DS + DB)))$$ (C.4)

Sediment Balance

$$AS = AW(DD + DT)/(DR + DT + DS + DB)$$ (C.5)

AW = Acivity of water
AS = Acivity of sedimet
AA = Acivity of air
AI = Acivity of water inflow
ABS = Bullk sediment Acivity Value
ABW = Bulk water acivity value
EW = Direct emissions
DB = Sediment Burial
DS = Sediment Transformation
DR = Sediment resuspension
DT = Sediment to water diffusion
DD = Sediment deposition
DW = Water Transformation
DV = Air to water absorption

DJ = Water outflow
DY = Water particle outflow
DM = Rain dissolution
DC = Wet particle deposition
DQ = Dry particle deposition
DI = Water inflow
DX = Water particle inflow

REFERENCES

1. ADINA,1995, *ADINA Software Manual*, ADINA Company, New York.

2. M. P. Anderson, K. W. Brown and J. Green, 1988. "Effect of Organic Fluids on the Permeability of Clay Soil Liners", *Report submitted to Texas A & M University.*

3. J. L. Aurialt and J. Lewandowska, 1996. "Diffusion/Adsorption/Advection Macrotransport in Soils", *European Journal of Soil Mechanics,* Vol. 4, No. 15, pp. 681 – 704.

4. D. A. Barry, 1997. "Factors Controlling the Distribution and Transport of Trichloroethene in a Sand Aquifer: Hydrogeology and Results of an In Situ Transport Experiment", *Journal of Hydrology*, Dec. 25, v 202, n1/4, page 315.

5. J. Bear and A. Verrujit, 1990, *Modeling Groundwater Flow and Pollution*, D. Riedel Publishing Company, AADordrecht, Holland, 1st Edition.

6. C. H. Benson, 1991. "Probability Distributions for Hydraulic Conductivity of Compacted Soil Liners", *ASCE Journal of Geotechnical Engineering*, Vol. 119, No. 3, pp. 471 – 486.

7. I. Bogard, W. E. Kelly and A. Bardossy, 1990. "Reliability Model for Soil Liner – Post Construction", *ASCE Journal of Geotechnical Engineering*, Vol. 116, No. 10, Oct., pp. 1502 – 1521.

8. J. J. Bowders and D. E. Daniel, 1990. " Hydraulic Conductivity of Compacted Clay Against Organic Chemicals", *ASCE Journal of Geotechnical Engineering*, Vol. 113, No. 10.

9. T. S. Bowers, N. S. Shifrin and B. L. Murphy, 1996. " Statistical Approach to Meeting Soil Clean up Goals", *Environmental Science and Technology*, Vol. 30, pp. 1437 – 1444.

10. G. P. Broderick and D. E. Daniel, 1990. "Stabilizing Compacted Clay against Chemical Attack", *ASCE Journal of Geotechnical Engineering*, Vol. 116, No. 10.

11. S. S. Chirputkar and Raghu D., 1998. "Risk Evaluation in Brownfield Slurry Wall Containments by Contaminant Transport and CalTOX Models", *ASCE, Risk Based Corrective Action*, Publication No. 82.

12. A. T. Corey, 1977, "Mechanics of Heterogeneous Fluids in Porous Media", *Water Resources Publication*, Fort Collins, Co, pp. 259.

13. M. Diamond and H.W.L. Lamprecht, 1996, "Loadings, Dynamics and Response Time of Seven Metals in Hamilton Harbor: Results of Mass Balance Study", *Water Quality Res., Journal of Canada*, Volume 31, No. 3, pp. 626-641.

14. M.I.J. Van Dijke, S.E.A.T.M. Van Zee and C.J. Van Duijn, 1995, "Multiphase Modeling of Air Sparging", *Advanced Water Resources*, Vol.26, pp. 186-193.

15. D. E. Daniel, 1993, *Geotechnical Practice of Solid Waste Disposal and Design*, Chapman and Hall, St. Edmunds, UK.

16. H. Y. Fang, 1997, *Introduction to Environmental Technology*, CRC Press, Boca Raton, USA.

17. D. E. Foreman and D. E. Daniel, 1986. "Permeation of Computed Clay with Organic Chemicals", *ASCE Journal of Geotechnical Engineering*, Vol. 112, No. 7, pp. 669 – 681.

18. D. G. Freudlund and H. Rahardjo, 1993, *Soil Mechanics of Unsaturated Soils*, John Wiley and Sons, Toronto, Canada.

19. D.G. Fredlund and H Rahardjo, 1993, "An overview of Unsaturated Soil Behavior", *ASCE Special Technical Publications on Unsaturated Soils*, No. 39, pp. 1-32.

20. R. Ghanem and S. Dham, 1995. "Stochastic Characterization in Multiphase Flow in Random Porous Media", *Proceedings of 3rd International Conference on Computer Methods in Water Resources*, pp. 315 – 322.

21. J.P. Giroud and R. Bonaparte, 1989, "Leakage through Liners Constructed with Geomembranes: Part 1Geomembrane Liners", *Geotextiles and Geomembranes*, 8, pp. 27-67.

22. K.E. Gustafson, 1980, *Partial Differential Equations*, John Wiley Sons, New York.

23. R. D. Holtz and W. D. Kovacs, 1981, *Introduction to Geotechnical Engineering*, Prentice Hall Inc., Englewood Cliffs, NJ.

24. S.L. Houston and W.N. Houston, 1997, "Collapsible Soils Engineering", *ASCE Special Technical Publication on Unsaturated Soils*, No. 68, pp. 199-233.

25. W. A. Jury, W. R. Gardener, W. H. Gardener, 1991, *Soil Physics*, John Wiley and Sons, New York, USA.

26. M. W. Kemblowski and H. A. Wajedasa, 1995. "Bayesian Decision Analysis for Contaminant Travel Time", *Risk Based Decision Making in Water Resources, Proceedings of 7th Conference*, Oct. 8 – 13.

27. A. Khandelwal and A. Rabideau, 1996. "Modeling of Diffusion Dominated Transport in Soil/Bentonite Slurry Walls", *Hazardous Industrial Waste, 28th Midatlantic Industrial and Hazardous Waste Conference*, pp. 134 – 141.

28. L. Lam, S.L. Barbour and W. A. Menely, 1979, "Seepage and Transport Modeling for a Uranium Tailing Dam in Northern Saskatchewan", *Canadian Journal of Geotechnical Engineering*, Vol. 23, pp.253-267.

29. A. Lehman 1979, *Geochemical Processes*, John Wiley and Sons, New York.

30. C. J. Leo and R. Booker, 1996, " A time stepping Finite Element Method for Analysis of Contaminated Transport in Porous Media", *International Journal for Numerical and Analytical Methods in Geomechanics*, Vol. 20, pp. 847 – 864.

31. S.C. Lim and K.J. Lee, 1992, "A Mass Conservative Numerical Solution of Vertical Water Flow and Mass Transport Equations in Unsaturated Porous Media", *Advanced Nuclear Energy*, Vol. 20, No. 2, pp. 91-99.

32. S.E. Manahan, 1989, *Toxicological Chemistry*, Lewis Publishers, Chelsea, Michigan, USA.

33. N.J. Meegoda and R.A. Rajapaske, 1993, "Short Term and Long Term Permeabilities of Contaminated Clays", *ACSE Journal of Environmental Engineering*, Vol. 119, No. 4, pp. 725-743.

34. N.J. Meegoda, R.T. Mueller, D.R. Huang, B.H. DuBose, Y. Chen and K.Y. Chuag, 1993, "Petroleum Contaminated Soils in Asphalt Concrete", *American Society for Testing and Materials, Special Technical Publications*, No. 1193, pp. 183-194.

35. M. Nakano, Y. Amemiya and K. Fuji, 1986, " Saturated and Unsaturated Hydraulic Conductivity of Swelling Clays", *Soil Science*, Vol. 141, No. 1, pp. 1-7.

36. Y. Nibori and T. Chida, 1994. "The Use of Standard Deviation and Skewness for Apparent Permeability in Two Dimensional, Heterogeneous Medium", *Transport in Porous Media*, Vol. 15, pp. 1 – 14.

37. D. Raghu and H. N. Hseih, 1988. "Chromium Contamination Problems", *Proceedings of Joint ASCE, CSCE National Conference on Environmental Engineering*, Vancouver, British Columbia, pp. 608 – 615.

38. D. Raghu and H.N. Hsieh, 1989, "Performance of Some Structures Constructed on Chromium Ore Residue Fills", *ASCE, Journal of Performance of Concrete Facilities*, Vol. 3, No. 2.

39. C. D. Shackleford, 1990. "Transit Time Design of Earthen Barriers", *Engineering Geology*, Vol. 29.

40. C. D. Shackleford and D. E. Daniel, 1991. "Diffusion in Saturated Soil I: Background", *Journal of Geotechnical Engineering*, Vol. 117, No. 3.

41. C. D. Shackleford and D. E. Daniel, 1991. "Diffusion in Saturated Soil II: Results for Compacted Clay", *Journal of Geotechnical Engineering*, Vol. 117, No. 3, March.

42. C. D. Shackleford, 1991. "Laboratory Testing for Waste Disposal", *Journal of Contaminant Hydrology*, Vol. 7, pp. 177-217.

43. C. Tachavises and C. H. Benson, 1997. "Hydraulic Importance of Defects in Vertical Groundwater Cutoff Walls", *Geotechnical Special Publication, Insitu Remediation of Geoenvironmental Engineering, Proceedings of ASCE National Fall Convention*, pp. 168 – 180.

44. G. J. Thoma, D. D. Relble, K. T. Valsaraj and L. J. Thlobodeux, "Efficiency of Capping Contaminated Sediment in situ - Mathematics of Diffusion-Adsorption in the Capping Layer", *Environmental Science and Technology*, Vol. 27, pp. 2412 – 2419.

45. U.S. Tim and S. Mostaghini, 1989, "Model for Predicting Transport of Pesticides and Their Metabolites in Unsaturated Zone", *Water Resources Bulletin*, Vol. 25, No. 4, pp. 765-774.

46. USEPA, 1989, *Risk Assessment Guidance for Superfund*; Volume I, Human Health Evaluation Manual.

47. USGS, 1993, "U.S. Geological Survey Toxic Substances Hydrology Program – *Proceedings of Technical Meeting, Colorado Springs*, September 20-24".

48. W. J. Weber and E. H. Smith, 1990. "Simulation and Design Models for Adsorption Processes", *Environmental Science and Technology*, Vol.116, No. 10.

49. R. Zhang and M.T. Van Genuchten, 1994, "Relative Hydraulic Conductivity: New Models for Unsaturated Hydraulic properties", *Soil Science*, Vol. 158, No. 2.

Electronic References:

1. Department of Toxic Substances, State of California, "CalTOX Manual", http://www.cwo.com/~herd1/caltox.htm, (2 Feb. 1999.).
2. Eco-Indiana, "Chromium", http://www.inetdirect.net/~ecoindy/chems/chromium.html, (3 Mar. 1999).
3. USEPA, 1998a, "Brownfields Glossary of Terms", http://www.epa.gov/swerops/bf/glossary.htm#brow, (2 Mar. 1999).
4. USEPA, 1998b, "Expediting Cleanup and Redevelopment of Brownfields: Addressing the Major Barriers to Private Sector Involvement.., Real or Perceived", http://www.epa.gov/epfinpage/brncle.htm#per1, (2 Mar. 1998).